

Viscoelastic & Mechanical Properties of the Carpal Tunnel Complex and Overlying Soft Tissue Layers



Mark Carter, BSc

A Masters project submitted in partial fulfilment of Msc degree, Bioengineering.

University of
Strathclyde

Bioengineering, Wolfson
Centre, Rottenrow,
Glasgow

Supervisor: Ukadike
Chris Ugbolue, PhD

Advisors: Philip Riches,
PhD, University of
Strathclyde and
Quentin Fogg, PhD,
University of Glasgow

16/08/2011

Declaration of Authorship

This thesis is the result of the author's original research. It has been composed by the author and has not been previously submitted for examination which has led to the award of a degree.

The copyright of this thesis belongs to the author under the terms of the United Kingdom Copyright Acts as qualified by University of Strathclyde Regulation 3.50. Due acknowledgement must always be made of the use of any material contained in, or derived from, this thesis.

Signed:

Date: 16/08/2008

Abstract

Background: Carpal Tunnel Syndrome (CTS) is a form of compression neuropathy of the median nerve as it passes through the carpal tunnel of the wrist. CTS is characterised by pain and paresthesia of the palm of the hand and the lateral three and a half fingers, muscular atrophy of the thenar and hypothenar muscles, leading to decreased grip and pinch strength, and decreased hand function. Severe and chronic cases of CTS often require open or endoscopic release of the transverse carpal ligament (TCL) for relief of carpal tunnel pressure. Techniques to stretch the TCL have been proposed but further understanding of the viscoelastic properties of the carpal tunnel complex is required.

Methods: Six embalmed cadaveric hands (82 ± 6.29 yrs) were tested in confined compression using a 10 mm diameter indenter at different levels of dissection (Intact, Skin and Adipose removed, thenar or hypothenar removed, and TCL exposed). Mean peak load, Load relaxation and Stiffness were recorded and compared between dissection levels using paired and unpaired t-tests.

Results: 'Skin removed' condition relaxed significantly quicker than 'Intact'. No other significant differences were found for load relaxation. Peak loads and stiffness generally increased with removal of each tissue layer. Significant differences were found for 'Intact' vs. 'TCL exposed' and the removal of the thenar muscle group resulted in greater peak loads and stiffness compared to removal of the hypothenar muscle group.

Conclusion: The skin and adipose layer ('Intact' condition) of the hand had the slowest relaxation times; while the muscular layer (Thenar muscle group) showed the fastest load relaxations, and greatest load absorption. Peak loads and stiffness generally increases for each layer of tissue removed. Testing at the 'TCL exposed' level with the test protocol used here does not isolate the TCL adequately to be able to attribute any mechanical or viscoelastic characteristics.

Table of Contents

Declaration of Authorship.....	2
Abstract.....	3
List of Tables	7
List of Figures	8
Acknowledgements.....	9
1 Introduction.....	10
1.1 Research Objectives.....	11
1.2 Background Information.....	11
1.2.1 Basic Anatomy of the Carpal Tunnel Complex	11
1.2.2 Skeletal Structure and Joints	12
1.2.3 Muscles and Tendons.....	12
1.2.4 Skin and Nerves	14
2 Review of the Literature	16
2.1 Introduction.....	16
2.2 Method	16
2.3 Discussion.....	17
2.3.1 Anatomy of the Human Wrist.....	17
2.3.2 Role of the Transverse Carpal Ligament	18
2.3.3 Mechanical and Viscoelastic Properties of Different Tissue Layers	20
2.3.4 Viscoelastic Properties of the Transverse Carpal Ligament	24
2.4 Conclusion	28
3 Methodology and Procedures.....	30
3.1 Subjects	30
3.2 Design	30
3.3 Materials	30
3.4 Procedure	31
3.4.1 Specimen Preparation and Dissection.....	32
3.4.2 Specimen Mounting	33
3.4.3 Test Protocol	33
3.5 Data Analysis	34

3.5.1	Calculation of Ligament Strain	35
3.6	Statistical Analysis	36
4	Results.....	37
4.1	Load Relaxation	39
4.1.1	Combined Group:.....	42
4.1.2	Hypothenar Group:	42
4.1.3	Thenar Group:	42
4.1.4	Between Group:	43
4.2	Peak Load.....	44
4.2.1	Combined Group:.....	44
4.2.2	Hypothenar Group:	44
4.2.3	Thenar Group:	44
4.2.4	Between group:	45
4.3	Stiffness.....	47
4.3.1	Combined Group:.....	47
4.3.2	Hypothenar Group:	47
4.3.3	Thenar Group:	47
4.3.4	Between Groups:.....	48
5	Discussion	50
5.1	Peak Load and Load Relaxation	51
5.1.1	Tissue layer differences	52
5.2	Stiffness.....	55
5.2.1	Tissue Layer Differences	56
6	Conclusion	58
6.1	De-limitations	58
6.2	Limitations	59
6.3	Future Recommendation.....	60
	References.....	61
	Appendix A: Material Photos	67
	Appendix B: Indenter Location Guide	68
	Appendix C: Dissection level Images.....	69
	Appendix D: Anderson-Darling Normality Tests.....	71
	Appendix E Homogeneity of Variance graphs	89

Appendix F: 95% Confidence Interval Graphs.....	91
Appendix G: Raw Anthropometric Measurements.....	94

List of Tables

Table 1: Anderson-Darling test for Normality (* unable to perform normality due to degrees of freedom = 1, ** contains an outlier).....	37
Table 2: Bartlett's Test for equal variance	38
Table 3: Mean \pm SD Peak Loads and Load relaxation results for the three test groups across all conditions	39
Table 4: t-test results for Relaxation Time (s) (M = Mean, SE = Standard Error)(* = Significant difference).....	43
Table 5: Paired t-test results for Peak Load (* Significant difference).....	45
Table 6: Paired t-test results and significance* values for stiffness.....	48
Table 7: Individual Specimen anthropometric measurements for the hand and wrist.	94
Table 8: Individual Specimen antropometric measurements; TCL dimensions	94

List of Figures

Figure 1: Simple 2D model of final ligament width: final ligament length is calculated from Pythagoras Theorum. Where: W_{CI} = half ligament width – half indenter width; I_D = Indentation depth; and I_W = Indenter width.	35
Figure 2: Normalised mean load relaxation graph for the Hypothenar Group; illustrating the similar viscoelastic properties at the different levels of dissection....	40
Figure 3: Normalised mean load relaxation graph for the Thenar Group.....	41
Figure 4: Normalised mean load relaxation for the Combined Group.....	41
Figure 5: Mean Peak loads and standard error for all dissection levels and groups. Illustrates the general increase in peak loads with each level of dissection.....	46
Figure 6: Mean stiffness with standard error across all dissection levels an groups. This graph illustrates the general increase in recorded stiffness at each subsequent level of dissection.....	49
Figure 7: Custom made 10 mm diameter aluminium indenter	67
Figure 8: Custom made aluminium specimen platform. Dimensions: overall width: 250 mm; length: 400mm; depth: 15mm; bolt grooves: 25mm indent from side, 300mm length, 8mm width. Restraining bars (x3): width: 32mm; length: 233mm; depth: 10mm. Bolts: 8mm threaded bolts with wing nuts.	67
Figure 9: Location of TCL centre of intact hand	68
Figure 10: Intact Hand with TCL centre located	69
Figure 11: Skin, subcutaneous adipose and palmar aponeurosis removed	69
Figure 12: Thenar Muscle Group Removed.....	70
Figure 13: TCL Exposed.....	70

Acknowledgements

I would like to take this opportunity to express my deepest gratitude to all those who have supported me in the completion of the Masters thesis.

Particular thanks go to my supervisor, Dr Chris Ugbolue, for his many hours of guidance and support.

I would also like to thank: my advisor, Dr Phillip Riches, for his invaluable technical knowledge; Dr Quentin Fogg, of the University of Glasgow for his anatomy knowledge; Thomas Harrison, for his mathematical acumen; and also to my wife, Gillian, and daughter, Bailey, for their patience and support throughout this Masters course.

1 Introduction

Carpal Tunnel Syndrome is a form of compression neuropathy of the median nerve as it passes through the carpal tunnel of the wrist. It is a painful and debilitating condition affecting approximately 4 to 12 people per 10000 of the UK population each year and is more prevalent in females than in males, with females accounting for approximately two thirds of total CTS cases, and more common in the over 40 age groups (NHS, 2010). CTS is characterised by pain, tingling, numbness and burning sensation of the lateral three and a half fingers, and palm of the hand; muscular atrophy of the thenar and hypothenar muscles, leading to decreased grip and pinch strength, and decreased hand function (Mathura *et al*, 2004; Gellman *et al*, 1989).

There are several possible causes of CTS including: tendonitis, tenosynovitis, bursitis, lesions and inflammation of the transverse carpal ligament. The effect of these is an increase of pressure within the carpal tunnel; compressing and impinging the median nerve.

Various conservative treatments may be prescribed to address the underlying cause of the condition, such as physical therapy, rest, nocturnal wrist splinting, non-steroidal anti-inflammatory drugs and corticosteroid injections. Surgical intervention to relieve carpal tunnel pressure is favoured where conservative methods have been unsuccessful or symptoms have persisted for six months or more. There are, predominantly, two surgical methods that are used to accomplish this: open-carpal release and endoscopic release, both with the end goal of increasing the available space within the carpal tunnel.

These methods involve complete transaction of the transverse carpal ligament. Open release surgery is the more traditional method and involves a 2 inch incision being made longitudinally over the palm and wrist with complete transaction of the palmar aponeurosis, flexor retinaculum and the transverse carpal ligament. The endoscopic release involves one to two incisions being made: one at the proximal wrist crease and another at the mid palm level. An endoscopic camera and an open top tube are inserted under the TCL, and a retrograde knife is used to transect the TCL only (Aroori and Spence, 2008).

Due to the invasive nature of these procedures complications are a risk and can include infection, damage to the median nerve, soft tissue fibrosis, stiffness and pain at the scar, loss of grip and pinch strength (Mathura *et al*, 2004), and wrist biomechanical abnormality (Kiritsis and Kline, 1995).

The risk of these complications has prompted the design of an alternative method for decompressing the carpal tunnel that avoids transection of the TCL so that wrist biomechanics and integrity are not unduly compromised. Berger (1993), proposed using a balloon catheter device inserted into the carpal tunnel and serially inflating and deflating the device to expand the carpal tunnel by stretching the TCL. Little research has been conducted into the efficacy of such a procedure and in particular the ability of the TCL to permanently elongate. Studies by Sucher (2005), Li *et al* (2009, 2011) and Holmes *et al* (2011) have investigated the mechanical properties of the TCL but do not investigate the viscoelastic properties of the TCL. Furthermore, little research has been conducted (Zheng *et al*, 2006) into the mechanical and viscoelastic properties of the soft tissue layers superficial to the TCL.

1.1 Research Objectives

The purpose of this study is therefore; to determine the mechanical and viscoelastic properties of the transverse carpal ligament and superficial soft tissue layers in the direction perpendicular to the palmar surface.

1.2 Background Information

1.2.1 Basic Anatomy of the Carpal Tunnel Complex

The carpal tunnel is a narrow passageway at the base of the hand comprised of a concave arch formed by the carpal bones to the posterior and sides with the TCL forming the roof on the palmer aspect. The carpal tunnel provides a conduit for the flexor tendons of the forearm and the median nerve. Annotated drawings of the wrist can be found in figures 1 and 2 at the end of this chapter.

1.2.2 Skeletal Structure and Joints

The hand and wrist is comprised of 27 bones: 8 carpals, 5 metacarpals and 14 phalanges. At the wrist the 8 bones of the carpus are divided into a proximal row and distal row (4 in each). The proximal row consists of the scaphoid, lunate and triquetral; with the pisiform sitting anteriorly to triquetral. The proximal ends of scaphoid and lunate articulate with the distal ends of the radius and ulnar to form the radiocarpal joint; while the distal end articulates with the proximal border of the distal carpal row. The distal row of the carpus is comprised of the trapezium, trapezoid, capitate and hamate and they articulate distally with the 5 metacarpals at the carpometacarpal joints (CMC). The trapezium articulates distally with the base of the first metacarpal; trapezoid with the second metacarpal; capitate with third and fourth metacarpals, and hamate articulates distally with fifth metacarpal. The 5 metacarpals each go on to articulate with the proximal phalanges of the fingers.

The carpus also forms a palmarly concave arch, called the carpal tunnel; walled on the ulnar side by the pisiform and hook of hamate, and on the radial side by the scaphoid and trapezium. The intercarpal joints are supported by strong intercarpal ligaments which provide stability and restricted intercarpal motion.

The transverse carpal ligament spans the 'roof' of the carpal tunnel; inserting radially into the tubercle of scaphoid and the ridge of the trapezium; and ulnarly into the hook of hamate, the pisiform and pisohamate ligament.

1.2.3 Muscles and Tendons

Extrinsic: The carpal tunnel provides a conduit for the passage of 9 flexor tendons (within the common flexor synovial sheath) and the median nerve from the forearm to the hand. The flexor tendons consist of: 4 tendons of flexor digitorum profundus, 4 tendons of flexor digitorum superficialis (encased in common ulnar sheath) and flexor pollicis longus (in radial sheath).

The tendon of flexor carpi ulnaris inserts into the base of the 5th metacarpal via the pisiform and the tendon of flexor carpi radialis passes through a fibro-osseous tunnel, on the radial aspect within the carpal tunnel, to insert into the base of the 2nd metacarpal.

Intrinsic: There are four groups of intrinsic hand muscles: the thenar and hypothenar muscles, the lumbrical muscles and the interossei muscles. The thenar group consists of abductor pollicis brevis, flexor pollicis brevis, opponens pollicis and adductor pollicis. The thenar group all have their origin on the radial aspect of the TCL and insert into the proximal phalanx of the thumb. The thenar muscles, with the exception of adductor pollicis, are innervated by the recurrent branch of the median nerve as it exits the carpal tunnel. The thenar muscles provide adduction, abduction, flexion and opposition of the thumb.

The hypothenar group consists of: abductor digiti minimi, flexor digiti minimi and opponens digiti minimi. Their origin is on the ulnar aspect of the TCL and insert into the base of the 5th proximal phalanx. All the muscles of the hypothenar group are innervated by the ulnar nerve and operate to perform flexion, abduction and opposition of the 5th metacarpal and phalange.

The lumbrical muscles are located deep in the palm of the hand. They originate from the tendons of flexor digitorum profundus, distal to the carpal tunnel, and insert into the radial aspect of the digital extensor tendons. The 2nd and 3rd lumbricals are innervated by the median nerve while the 4th and 5th are innervated by the ulnar nerve.

The interossei muscle consist of 3 palmar and 4 dorsal muscles. They originate from the two borders of the metacarpals between which they sit and insert into the proximal phalanges of the 2nd to 4th digitis. They act to adduct and abduct the fingers and are all innervated by the ulnar nerve.

Superficial to the TCL and palm of the hand lays the palmar aponeurosis and its tendon, Palmaris longus. Palmaris longus is absent in approximately 15% of the population, but where present, it inserts into the palmar fascia of the hand before dividing into slips attaching to the palmar skin of each finger (2nd to 5th).

1.2.4 Skin and Nerves

Two main nerves pass into the hand; the ulnar and median nerves. The ulnar nerve passes into the hand external to the TCL via the ulnar canal. The median nerve passes into the hand through the carpal tunnel to provide motor function and sensation for the radial aspect of the palmar hand. The palmar skin is thick with strong attachments to the underlying palmar fascia. The palmar creases of the hand indicate the strongest attachments of the skin to the underlying tissue. A layer of subcutaneous adipose can also be found across much of the palmar surface to provide shock absorption. (Agur and Dalley, 2009; Yu *et al*, 2004).

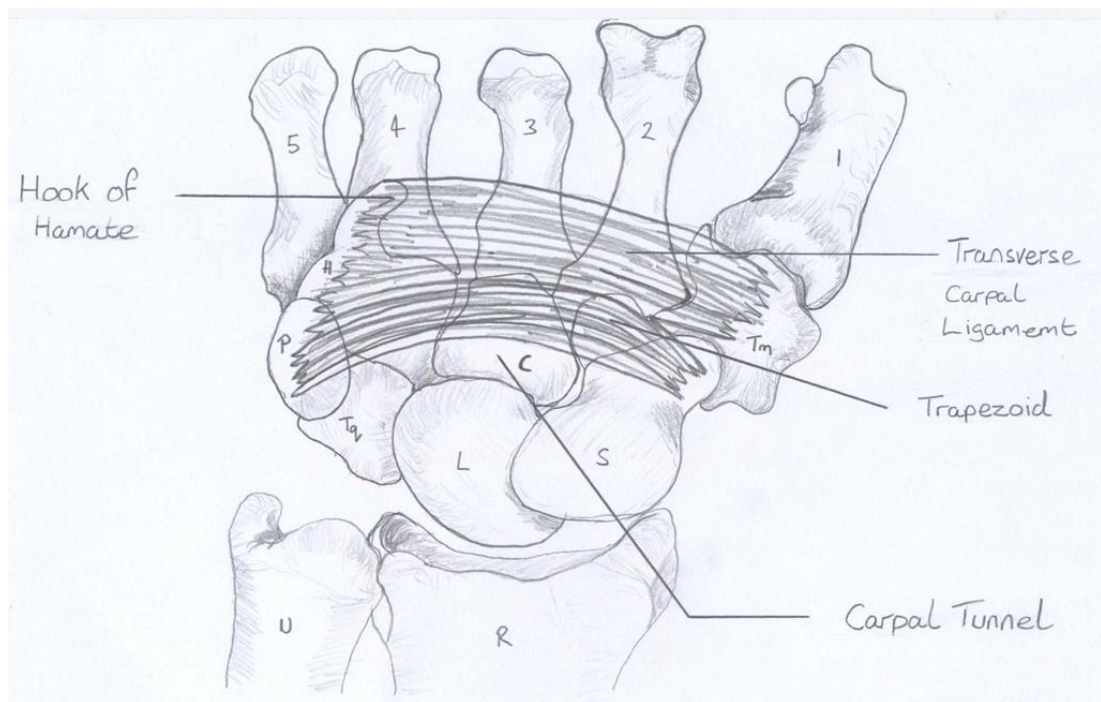


Figure 1: Transverse Carpal Ligament

Key:

- | | |
|-------------------------------|-------------------|
| 1. 1 st metacarpal | H. Hook of Hamate |
| 2. 2 nd metacarpal | C. Capitate |
| 3. 3 rd metacarpal | Tm. Trapezium |
| 4. 4 th metacarpal | P. Pisiform |
| 5. 5 th metacarpal | Tq. Triquetrum |
| | L. Lunate |
| | S. Scaphoid |
| | U. Ulna |
| | R. Radius |

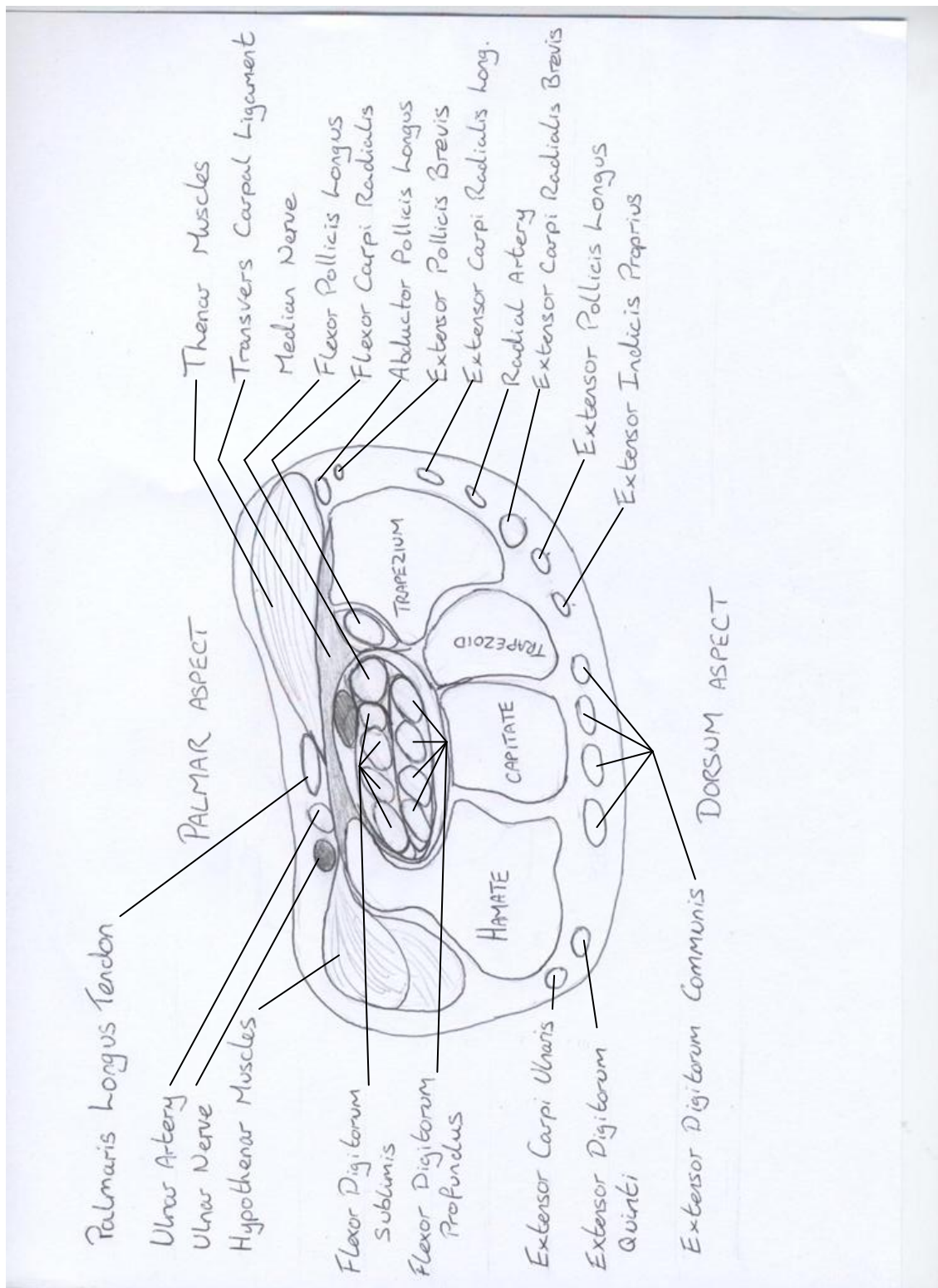


Figure 2: Anatomy of the wrist at the level of distal carpal tunnel

2 Review of the Literature

2.1 Introduction

The mechanical and viscoelastic properties of human soft tissue has been investigated extensively and there are numerous studies into carpal tunnel syndrome; aetiology, methods of treatment, their efficacy, carpal tunnel mechanics and many more. Berger (1993) proposed a method of elongating the TCL, as opposed to transection, as a treatment method to relieve pressure within the carpal tunnel and to avoid many of the post-operative complications associated with open and endoscopic release surgery. Some research has been conducted into the validity of this idea, and one key factor requiring investigation is the viscoelastic properties of the TCL. This review of the literature, therefore, aims to explore the research previously conducted on wrist biomechanics, soft tissue mechanics and ligament viscoelasticity; to give the reader a full understanding of the current field of knowledge of this subject and to highlight where more work is required.

2.2 Method

Online internet searches were performed using PubMed central, ISI Web of Knowledge and Google Scholar for studies published in English between 1980 and 2011. The following keywords were used in the search, either alone or in any combination: Transverse carpal ligament, viscoelastic, carpal tunnel syndrome, percutaneous carpal tunnel plasty, mechanical properties, stiffness, stress/load-relaxation, and confined compression. 34 journal articles have been reviewed in this paper.

2.3 Discussion

2.3.1 Anatomy of the Human Wrist

There has often been some ambiguity with regard to the use of the terms *flexor retinaculum* and the *transverse carpal ligament* to describe the structure that forms the roof of the carpal tunnel; uniting the four marginal bones of the carpus and serving as an insertion for the thenar and hypothenar muscle groups. Previously, these terms have both been utilised to describe the same structure even though their fundamental definitions differ. A ‘retinaculum’ is a structure that retains an organ or other tissue in place, while a ‘ligament’ is defined as a band of fibrous tissue that connects bone to bone (or cartilage) and supports joints (Medical dictionary, online, 2011)

Grant’s Atlas of Anatomy (11th edition, Agur and Dalley, 2009) does not make any distinction between the flexor retinaculum and the transverse carpal ligament indicating they are one and the same structure while Middleton *et al* (1987) refers to this structure only as the flexor retinaculum. Cobb *et al* (1993) investigated 26 cadaveric arms via histological and radiographical methods and proposes there to be three distinct but contiguous segments to the flexor retinaculum: a proximal deep investing fascia of the forearm; the transverse carpal ligament spanning the carpal arch; and a distal portion of aponeurosis between the thenar and hypothenar muscle groups.

Stecco *et al* (2010) also performed a cadaveric study to more accurately differentiate the flexor retinaculum and the transverse carpal ligament. In their study, 30 unembalmed hands were examined by dissection and histological, and immunohistochemical staining. They found there to be two distinct structures on the volar aspect of the wrist: the antebrachial fascia, being composed of three layers of undulating collagen fibre bundles with different fibre orientations between layers, many nerve fibres and Pacini and Ruffini corpuscles. Deep to this fibrous layer another fibrous structure was identified; comprised of thicker fibre bundles with few nerve fibres, and spanning the carpal arch between the pisiform and hook of hamate on the ulnar side to the tubercle of scaphoid and ridge of trapezium on the radial side.

The researchers concluded that the superficial tissue is in continuity with the antebrachial fascia and acts as its reinforcement while the deeper structure is characteristic of ligamentous tissue and connects the four marginal bones of the carpus together. They propose that the term transverse carpal ligament be used to describe the lamina of tissue connecting the pisiform and hook of hamate to the trapezium and scaphoid, while the term flexor retinaculum should be abandoned as it does not relate to a specific structure.

2.3.2 Role of the Transverse Carpal Ligament

Some of the previous ambiguity in the terminology of the structure covering the carpal tunnel can be attributed to the role the TCL in wrist and hand biomechanics. The TCL has two main roles in wrist function: carpal arch stability and retention of the extrinsic digital flexor tendons within the carpal tunnel for effective wrist biomechanics.

The TCL is important in the stability of the carpus. A study by Xiu *et al* (2010) investigated the structural mechanics of the carpal arch and the TCL. They applied paired forces to the attachment sites of the TCL (two forces applied to the pisiform and hook of hamate on the ulnar side and two forces applied to the scaphoid and trapezium on the radial side). Carpal tunnel and carpal arch deformation was compared with the TCL intact and transected; with both inwardly and outwardly applied loads. They report that under 10N of inwardly applied load with the TCL intact, carpal arch width decreased by 10.8% at the distal portion and by 37.5% at the proximal portion. With the TCL transected the same test resulted in a decrease of 10.6% and 37.9% distally and proximally respectively. When an outwardly applied load of 10N was placed with the TCL intact, carpal arch width increased by 3.7% distally and 18.8% proximally. While following TCL transection increases of 9.6% distally and 33.9% proximally were reported. The authors concluded that the TCL plays an important role in the stabilisation of the carpal tunnel under outwardly applied loads and that the proximal portion of the carpal arch is more compliant than the distal portion.

The findings reported by Xiu *et al* (2010) support those of a similar study by Tengrootenhuysen *et al* (2009) who found that gradual sectioning of the TCL resulted in significant increases in carpal arch width while under load. However, the authors of this study stated that the carpal arch retains a good level of stability after transection of the TCL.

Grip and pinch strength can also be affected following transection of the TCL. A study by Gellman *et al* (1988) evaluated the length of time required following carpal tunnel release surgery for grip and pinch strength to return to preoperative levels. They found that grip strength returned to preoperative levels by 3 months post-operation and that by 3 weeks and 6 weeks grip strength was 28% and 73% respectively. Pinch strength was found to return sooner with 74% and 96% recovery by weeks 3 and 6 respectively and 108% by 3 months.

Grip strength was also analysed by Mathura *et al* (2004). In this study, 30 patients with carpal tunnel syndrome were tested for power grip and key pinch strength with the wrist extended and flexed, and before and after carpal tunnel release surgery. There were no reported differences in key pinch strength; however there was a significant decrease in grip strength following carpal tunnel release in both wrist extension and flexion with the greatest decrease evident during wrist flexion. The authors attribute the loss of grip strength during wrist flexion to excursion of the flexor tendons out of the carpal tunnel.

The excursion or 'bow-stringing' of the flexor tendons against the palmar surface of the hand during wrist flexion has been documented in some earlier studies (Kline and Moore, 1992; Kiritsis and Kline, 1995). Kline and Moore (1992) examined four fresh-frozen cadaver hands for flexor tendon excursion during extension and flexion of the wrist before and after TCL transection. Following transection of the TCL, tendon excursion palmarly during wrist flexion was found to increase by 25% and 20% for the tendons of digitorum profundus and digitorum superficialis respectively. This equated to a 'bow-stringing' displacement of 5.4 ± 1.2 mm and 5.5 ± 1.3 mm respectively. The authors propose that the TCL acts to maintain the flexor tendons close to the centre of rotation of the radiocarpal, intercarpal, and carpometacarpal joints; creating an effective pulley system. Transection of the TCL disrupts this flexor pulley system and palmarly directed excursion of the tendons during flexion

limits the available motion at other joints where these tendons act. The authors also state that this may contribute to the loss of grip strength experienced following carpal tunnel release surgery.

2.3.3 Mechanical and Viscoelastic Properties of Different Tissue Layers

If ligament elongation is chosen over transection as a treatment method, it would be necessary and prudent to consider not only the viscoelastic properties of the TCL but also those of the tissue layers and structures superficial to the TCL. Anterior to the TCL, the flexor retinaculum and the attaching fibres of the thenar and hypothenar muscles can be found. Above this layer, in the majority of individuals, lays the palmar aponeurosis and its tendon, Palmaris longus. Anteriorly to this lies the subcutaneous adipose layer followed by the dermal and epidermal layers of the skin.

Various studies have been conducted to investigate the mechanical properties of the skin layers (with various results reported). An older study by Agache *et al* (1980) looked at the mechanical properties of the dermis in vivo using a rotating disc (enclosed in a guard ring) to apply a fixed amount of torque to the skin. A torque of 28.6 Nmm was applied to the dorsal skin of the forearm of 138 volunteers, aged 3-89 years. The researchers report Young's Moduli of 0.42 and 0.85 Mpa for young and older age groups respectively (<30 yrs: >30 yrs). The researchers also report that elasticity of the skin remains stable until the age of 30 years where it drops by approximately 50%, while Young's Modulus follows an inverse pattern whereby it increases by approximately 50% around the age of 30 years.

Smalls *et al* (2006) reports some similar findings in their study. They looked at the effect of dermal thickness, body site and tissue composition on the biomechanical properties of healthy female volunteers using a negative pressure (suction) method. The researchers report significant correlations for skin thickness to stiffness, energy absorption and biological elasticity (ratio of elastic recovery to elastic deformation). They also report differences between body sites. Stiffness was found to be significantly higher at the calf compared to the thigh and shoulder; and significantly

higher at all sites on the dominant side compared to the non-dominant side. Age was found to be a factor. Significant decreases in elasticity were found for increases in age; however, no increase in stiffness was found at any site with age; a finding that contradicts those of Agache *et al* (1980) but may be due to the different methodologies employed between the two studies.

A more recent study by Chrichton *et al* (2011) employed yet another technique to measure the viscoelastic properties of the skin. The researchers here used Atomic Force Microscopy (AFM) indentation on mouse skin layers using two different sized spherical nano-indenters. They compared a 6.62 μm indenter to a 1.9 μm indenter on the elastic moduli and stress relaxation of the stratum corneum (SC), viable epidermis (VE) and the dermis of mouse ear skin. They report significantly greater stiffness values for the dermis (7.33 – 13.48 MPa) compared to the SC (0.75 – 1.62 MPa) and VE (0.49 – 1.51 MPa. The lower – larger values represent the larger – smaller indenter results respectively). They also found the VE to show the greatest amount of relaxation; almost fully relaxing within 10 seconds. The SC and dermis in comparison, both relaxed initially before reaching a plateau at approximately 40% relaxation. The researchers postulate that the higher stiffness values for the dermis compared to the other layers may be due to the higher collagen and elastin content of the dermis preventing rapid expulsion of fluid. The shorter term viscoelasticity of the SC layer is thought to be due to the hydration gradient found between the superficial surface (15%) and the SC/VE boundary layer (70%). The author proposes that the dryer, rigid surface of the SC allows stress distribution of the indenters and that the higher fluid content and lower cellular matrix density of the VE allows faster fluid expulsion compared to the other layers.

Lying deep to the dermis is the hypodermis, also known as the subcutaneous tissue, is a layer consisting of loose connective tissue housing lobules of adipocytes and other cells such as fibroblasts and macrophages. The hypodermis is found at all sites of the body and the subcutaneous adipose found within the hypodermis primarily acts as a layer of thermal insulation and energy storage. There are sites of the body that require fat pads for purposes other than previously mentioned. The adipose tissue found in the calcaneal and palmar fat pads are responsible for shock absorption

and load bearing. This results in a different chemical composition of the adipose at these sites compared to the rest of the body's subcutaneous adipose. The fat pads of the hands and feet have a larger ratio of unsaturated to saturated fatty acids (Geerligs *et al*, 2008).

Geerligs *et al* (2008) investigated the linear viscoelastic properties of porcine subcutaneous adipose using rotational rheometer methods. They reported a shear modulus of 7.5 kPa at 10 rad/s and 37°C. They also looked at the effects of snap freezing and report that the mechanical properties of the tissue did not change even though some cell damage was evident under histological examination. The researchers also reported that the storage and loss modulus at up to 0.1% strain showed strain rate and temperature dependency. A more relevant study by Miller-Young *et al* (2002) performed unconfined compression tests on human calcaneal fat pad samples to determine its material properties. Cylindrical sections ~ 10 mm thick and 8 mm in diameter were tested with instantaneous compression to 40% strain. The researchers report peak stresses of 21.3 kPa relaxing to 5.4 kPa after 60s. A strain rate dependence on peak stress was also found here with peak stresses of 33.7 and 25.2 kPa being recorded for displacement rates of 350 mm/s and 175 mm/s respectively. The author explains that the structure of the fat pad; with its high ratio of unsaturated fatty acids, may explain the rapid stress relaxation. They state that due to unsaturated fatty acids being highly branched they are able to move quite freely, and combined with a reduced intercompartment fluid flow, results in a less viscous material. These finding may be relevant since the palmar fat pad is similar in its composition to the calcaneal fat pad.

The layer of soft tissue anterior to the TCL is comprised of myocytes (muscle fibres) of the thenar and hypothenar muscles and their tendinous fibres as they converge with the TCL and each other. Skeletal muscles are generally connected to bones on either side of one or more articular joints to provide movement and postural support. They are connected either directly or indirectly to the bone via continuation of the collagenous fibres of the muscles endomysium, perimysium and epimysium with those of the periosteum of the bone. An indirect attachment implies there is a gap between the muscle fibres and the bone that is bridged by the convergence of the

muscular fascias into tendinous fascicles which then continue into the periosteum. The origin of the thenar and hypothenar muscles is considered to be the carpal bones via the TCL (Agur and Dalley, 2009). However, Tanabe and Okutsu (1997) found that the originating fibres of the thenar and hypothenar muscles attach to each other; forming a layer of transverse fibres separate and slightly distal to the TCL. Whether these fibres originate from the TCL or not, they are still an important component in wrist and hand biomechanics, and also in the mechanics of carpal tunnel syndrome. For effective relief of CTS, decompression of the carpal tunnel is required and this is usually accomplished through transection of the TCL. Tanabe and Okutsu (1997) examined 20 cadaveric hands and found that the distance between the cut ends of the TCL increased from 1.5 mm to 6.6 mm when the transverse fibres between the thenar and hypothenar muscle were also severed. Their results suggest that the attaching fibres of the thenar and hypothenar muscles play a role in carpal tunnel mechanics and may add to the structural integrity provided by the TCL.

The point of attachment of the tendinous fibres of these two muscle groups along the TCL may differ among individuals, along with the extent to which the muscle fibres traverse the TCL (Dr Q Fogg, personal communication, 2nd June 2011). Since the thenar and hypothenar muscles also contribute to load bearing and shock absorption over the TCL, their mechanical and viscoelastic properties should also be considered.

Van Loocke *et al* (2008) investigated the viscoelastic properties of passive skeletal muscle. They performed uniaxial unconfined compression and hold tests on fresh porcine skeletal muscle at different fibre orientations (along fibres, cross-fibre and 45° fibre angle) and deformation rates. Both the rate of deformation and the fibre orientation during ramped compression were found to be factors in the stiffening effect of the muscle. Greater stiffness was observed cross-fibre at low strain rates (<5% s⁻¹), while above this strain rate, stiffness was greatest when the fibre orientation was parallel to the direction of compression. Stress relaxation was greatest for the parallel fibre direction (60% relaxation) compared to cross-fibre compression (45% relaxation) but in all cases, 80% of the stress relaxation occurred within the first 100 s. The rate of relaxation was shown to only be affected by the amount of compression and not the rate of compression. No significant differences

were reported for relaxation rate due to compression rate but a drop from 30% to 10% deformation resulted in a 20% increase in relaxation rate. The difference in viscoelastic behaviour due to the fibre orientation, therefore, results in the skeletal muscle being anisotropic.

The stress relaxation reported by Van Loocke *et al* (2008) is slightly less than that reported in an earlier study by Silver-Thorn (1999) as noted by the authors of the more recent study. Silver-Thorn (1999) reported *in-vivo* force relaxations of 55-95% on the soft tissue bulk of the calf of trans-tibial amputees and non-amputees, with equilibrium being reached within 60 s, quicker than that reported by Van Loocke *et al* (2008). However, there are major methodological differences between the two studies that may account for the difference.

2.3.4 Viscoelastic Properties of the Transverse Carpal Ligament

Ligaments are a viscoelastic material, in that their behaviour is time-dependent. These responses include stress relaxation and creep. When a ligament is held at a constant strain the stress experienced by the ligament decreases with time (stress relaxation), and conversely, when a ligament is held with a constant level of stress the ligament elongates with time (creep). Further to these definitions, the stress relaxation of ligaments is said to be strain dependent. Duenweld *et al* (2009) found that the rate of relaxation in tendons is dependent on the level of strain and that as strain increases; the rate of relaxation also increases. This contradicts the finding of Van Loocke *et al* (2008) which reports faster relaxation rates in muscle with lower levels of strain. An explanation to this discrepancy may be found in the structural and compositional differences of muscle and tendinous tissue. Bonifasi-Lista *et al* (2005) found that stress relaxation progressed faster at lower strain levels in human medial collateral ligaments, and that energy dissipation was greatest at high strain levels. The author attributes this to the uncrimping of the collagen fibres during low-level strains; the solid constituents of the MCL are less involved at low strains and that the ground substance matrix (glycosaminoglycans (GAG), proteoglycans (PG) and water) is more viscous in character and bears the majority of the load.

Provenzano *et al* (2001) also found relaxation rate to decrease with increasing strain in the MCLs of rats. The researcher here posited that at higher strains, a greater amount of fluid is expelled from the tissue making the tissue more elastic. Therefore, water content affects relaxation with higher water content in ligaments resulting in greater levels of load relaxation (Chimich *et al*, 1992).

There is an abundance of research conducted into the viscoelastic properties of ligaments, especially those of the knee, however, ligament function varies by location as does its composition and structure, as Frank (2004) suggests. Specific research into the viscoelastic properties of the TCL is much scarcer. Studies have been carried out on the extensibility of the TCL and/or the expansion of the carpal tunnel.

Sucher *et al* (2005) investigated transverse carpal arch (TCA) width under static and dynamic loading. The static loading comprised of 10 N loads being applied to pins inserted in the four (TCL attaching) carpal bones and the TCA width was measured over 3 hours, after which the load was removed and the TCA allowed to recover. Measurements were also taken during the 2 hour recovery. Dynamic loading consisted of a series of osteopathic manipulations being applied to the hands prior to static loading as above. Their results showed that under static loading, the TCL elongated by approximately 3.7 mm (13%) and recovered to an elongated length of 2.6 mm. The dynamic loading condition resulted in an even greater elongation after the static load, as would be expected. The research also found that female hands were more compliant than those of males; while a study by Li (2005) found the carpal tunnels of females to be less compliant than those of males. In the latter investigation, manual indentation of the TCL region, perpendicular to the palmar surface of 12 male and 12 female volunteers was performed. With load increases from 0.25 kg to 2.00 kg, indentation depths of 1.82 ± 0.30 mm and 1.38 ± 0.25 mm were recorded for males and females respectively. This equated to an effective compliance of 0.101 ± 0.018 mm/N for males and 0.075 mm/N for females (24.5% less). The researcher posited that this may be a factor for the greater prevalence of CTS in females. This may suggest that the carpal tunnels in females are less compliant due to their smaller size compared to males. Bower (2006) in an MRI

investigation into CT dimensions, found males had significantly larger carpal tunnels and carpal tunnel contents than females, but there was no difference in 'CT': 'CT content' ratio between males and females. The research also found that the cross-sectional area of the carpal tunnel was smallest at the distal end (level of hook of hamate) especially during wrist flexion.

A smaller volume of the carpal tunnel may result in greater carpal tunnel pressures associated with CTS, with an average of 36 mmHg being reported by Uchiyama *et al* (2010). An increase in carpal tunnel pressure can be the result of numerous causes; mostly inflammatory pathologies of various structures associated with the carpal tunnel complex. Another cause that may be a factor in repetitive stress related CTS is the incursion of the lumbrical muscles into the carpal tunnel during finger flexion. Cobb *et al* (1993) measured the extent to which the lumbrical muscles were pulled into the carpal tunnel on five cadaveric hands. The lumbrical muscles have their origin on the tendons of flexor digitorum profundus in the palm of the hand. The researcher found that the origins of the lumbrical muscles translated from 7.8 mm distal to the TCL, at full finger extension, to 30 mm within the tunnel at 100% finger flexion.

A method of elongating the TCL, as opposed to transection, was developed by Berger (1993) using an inflatable balloon catheter that could be inserted under the TCL and then inflated to palmarly stretch the TCL. The device also incorporated a nerve shield to lessen the pressure exerted on the median nerve during the procedure. To validate the efficacy of this procedure, proper understanding of the mechanics of the carpal arch and TCL are needed.

Zheng *et al* (2006) used a Tissue Ultrasound Palpation Sensor (TUPS) to measure the thickness and elasticity of the tissue in the carpal tunnel area of five male volunteers. They report average tissue thicknesses overlying the TCL of 7.98 ± 1.05 mm and a tunnel depth of 9.59 ± 1.12 mm (with 5 N loads and a 9 mm diameter indenter). The stiffness of the soft tissue layer above the TCL was reported as 6.72 ± 2.10 N/mm and 15.63 ± 8.42 N/mm for the tunnel contents. The author also posited that that the stiffness may be affected by the boundary conditions: a small tunnel would provide

less available space to accommodate deformation of the tunnel contents; resulting in greater apparent stiffness.

A study by Li *et al* (2009) looked at the ability of the TCL to stretch from a palmarly applied load from within the carpal tunnel. The hands of ten fresh frozen cadaveric specimens were tested in this investigation. The dissected hands were secured and a lever inserted into the excavated carpal tunnel. Loads of 10 N to 200 N were applied to stretch the TCL palmarly. The researchers found that length of the TCL did not change during loading but formed an arch, pulling in the side walls of the carpal tunnel. The researchers report that under a 10 N load the carpal tunnel area (CTA) increased by $33.3 \pm 5.6 \text{ mm}^2$ from a resting area of $148.4 \pm 36.8 \text{ mm}^2$ (22.4% increase), and by $48.7 \pm 11.4 \text{ mm}^2$ under 200 N of load (32.8% increase). The author concludes that since there was no elongation of the TCL, the increase in CTA was due to changes in shape of the tunnel; carpal arch width decreased and tunnel depth increased. A more recent Study by Li *et al* (2011) incorporated a similar method to increase CTA but utilising a balloon device inflated in the carpal tunnel with precise amount of pressure. In this investigation they found that the cross-section area at the hook of hamate level increased by 9.2% with 100 mmHg of pressure and by 14.8% with 200 mmHg. Again, the author notes that the circularity of the carpal tunnel increases during the procedure rather than any actual elongation of the TCL.

Elongation of the TCL may still be possible though. A study by Holmes *et al* (2011) investigated the effects of wrist posture and indenter size on the mechanical properties of ten fresh frozen, exposed TCL (*ex vivo*) and the carpal tunnel (carpal tunnel contents intact) complexes. Here, perpendicular indentation of the TCL was performed using four different sized indenters (5, 10, 20 and 35 mm diameters) and in three different wrist postures (neutral, 30° flexion and 30° extension) to measure the resulting displacements from a 50 N load applied at a rate of 5 N/s. The researchers report that the flexed wrist posture resulted in significantly greater stiffness ($40.0 \pm 3.3 \text{ N/mm}$) than neutral ($35.9 \pm 3.5 \text{ N/mm}$) and extended ($34.9 \pm 2.8 \text{ N/mm}$) positions. Stiffness was found to be significantly greater for the 10 mm and 20 mm indenters compared to the 5 mm indenter, while the 35 mm indenter produced significantly less stiffness than the 20 mm indenter only. Also of interest, and in

contrast to the findings reported by Li *et al* (2009 and 2011), was that there was no significant decrease in carpal arch width reported between peak loading (28.7 ± 0.4 mm) and at rest (29.3 ± 0.5 mm). However, the different methodological approaches to testing the carpal tunnel complex between these two studies may account for the difference. Holmes *et al* (2011) postulates that the ratio of indenter size to ligament width may affect the stiffness. Since the radial and ulnar portions of the TCL have been found to be thicker at the radial and ulnar edges (Pacek *et al*, 2010), the wider indenters (apart from the 35 mm indenter) will encroach on these thicker portions of the TCL to a greater degree than a narrow indenter.

While the study by Holmes *et al* (2011) does not address the viscoelastic properties of the TCL, the results are of interest. A similar short study by Chaise *et al* (2003) does investigate the viscoelastic properties of the TCL, but only from one fresh frozen hand (81 yr old male). Indentation was performed using a 10 mm indenter at three levels of dissection: on the palmar surface, on the exposed TCL with tunnel contents intact, and on the exposed TCL with the tunnel contents removed. Cyclic preconditioning (0-6 mm at 2 Hz for 5 min) was applied before each of 3 trials of ramp and hold displacement (8 mm, held for 30 min) and for 3 trials of cyclic load relaxation (0-8 mm at 2 Hz for 10 min) at each dissection level. A 1 hour recovery period between trials was included. The peak load recorded for the palmar surface, TCL-exposed and TCL-only conditions were 27.1, 80.5 and 21.7 N respectively. The stiffness of the TCL –exposed condition (46.0 N/mm) was reported to be approximately three times greater than the other two conditions (palmar surface: 15.6 N/mm, and TCL-only: 10.1 N/mm) for the ramp and relaxation test.

The present study employed a very similar methodology to that used by Holmes *et al* (2011). Indentation was performed with a 10 mm indenter, in a neutral wrist posture only, indentation was controlled by displacement (6 mm for preconditioning and 8 mm for ramp and hold test) and the specimen was subjected to an extensive number of trials.

2.4 Conclusion

Following a review of the literature, it can be seen there are many different wrist structures that need to be considered when treating CTS. The various testing protocols and methodologies used to investigate soft tissue mechanics across these studies impose limitations on the ability to directly compare the results.

When testing the mechanics of the TCL, few researchers employ the same methodology of testing. Tensile methods have been used by Li *et al* (2009, 2011) while indentation methods have been utilised by Holmes *et al* (2011) and Chaise *et al* (2003). Regardless of the test methodologies used, there is still a lack in research into the viscoelastic properties of the TCL with little consideration given to the mechanical and viscoelastic properties of the tissues superficial to the TCL.

3 Methodology and Procedures

3.1 Subjects

Six embalmed cadaveric hands, amputated at the mid forearm level, were tested in this investigation (82 ± 6.29 years of age). The six hands were from four individuals (two pairs and two individual hands), three male (four hands) and one female (both hands). All cadaveric specimen donors have no history of injury or pathology of the wrist. The specimens were supplied by the Laboratory of Human Anatomy, University of Glasgow.

3.2 Design

The viscoelastic and mechanical properties of the intact TCL were tested in compression (indentation) using a materials testing machine.

Four indentation trials for each specimen at different levels of dissection were performed to compare the mechanical and viscoelastic properties between conditions and to compare the individual effect of the thenar and hypothenar muscle groups on the measured variables.

There are two independent variables: Group; with three levels (Thenar group, Hypothenar group and Combined); and Condition; with four levels (Intact, Skin removed, Hypothenar or Thenar removed, and TCL exposed). There are three dependant variables of interest: Peak Load (N), 80% Load Relaxation Time (s), and Stiffness (N/mm).

3.3 Materials

Cadaveric specimens were transported in secure, leak proof, and appropriately labelled containers from the Laboratory of Human Anatomy, University of Glasgow

to the Level II containment suit of the Bioengineering department, University of Strathclyde, Glasgow.

Anthropometric measurements, such as: wrist width, wrist depth, palm width and palm depth (at the carpus and at the distal metacarpus), and TCL width, length and thickness were recorded for all specimens using digital precision callipers (Mitutoyo Digimatic).

Dissection was performed using standard dissection tools: forceps, scalpel, and scissors. The researchers donned appropriate protective laboratory coats and blue nitrile gloves when handling and testing the cadaveric specimens.

Indentation was performed using a custom made 10 mm diameter aluminium indenter (fig. 7, Appendix A). Indentation was performed using a BOSE ElectroForce 3200 materials testing machine with a BOSE 450.00 N dry load cell (model: 10-32 THD) fitted in series between the indenter and the upper actuator of the machine. The testing machine was operated by personal computer (PC) running Wintest 4.1 Digital Control System software package.

The cadaveric hands were secured to a custom built aluminium plate that was fixed to the base of the testing machine (fig. 8, Appendix A). The specimens were secured in place via three rectangular aluminium bars that could be tightened down via two 8 mm diameter threaded bolts and wing nuts per bar.

3.4 Procedure

Six specimens were each tested in four indentation trials:

1. Intact hand
2. Skin removed: epidermis, dermis, subcutaneous adipose and palmar aponeurosis removed
3. Removal of one muscle group (thenar or hypothenar)
4. TCL exposed (removal of remaining muscle group to fully expose the TCL, with carpal tunnel contents intact)

One specimen was tested in a fifth trial following removal of the carpal tunnel contents (TCL Only) to give a single comparison of the effect of the tunnel contents on stiffness and load relaxation.

3.4.1 Specimen Preparation and Dissection

Prior to testing, anthropometric details were recorded for each specimen and the centre of the TCL was located and marked for accurate indenter placement. Measurements were taken for wrist width, wrist thickness, palm width (carpal level), distal palm width, and palm thickness at the mid TCL level.

The centre of the TCL on the intact hand was determined through palpation and marking of the pisiform and hook of hamate ulnarly and the tubercle of scaphoid and ridge of the trapezium radially. Two transverse lines were drawn: one distal connecting the hook of hamate to the first carpometacarpal joint, and one proximal connecting the pisiform to the tubercle of scaphoid. A longitudinal line was then drawn following the radial side of the fourth phalange and intersecting both transverse lines. The centre of the TCL was identified as a point on the longitudinal line 10 mm proximally from the distal transverse line (Appendix B).

Following each trial the specimens were dissected in preparation for the next trial. After trial one, all specimen were carefully dissected to remove the skin, subcutaneous adipose, the palmar aponeurosis and palmaris longus tendon, and palmaris brevis muscle. The centre of the TCL was then relocated and marked using the above procedure.

Upon completion of trial two (skin removed) three specimens were dissected to remove the thenar muscles (leaving the hypothenar muscles intact) and three were dissected to remove the hypothenar muscles (leaving the thenar muscles intact).

Trial three was then performed with three specimens in each group (thenar removed, and hypothenar removed).

Following the third trial the remaining thenar or hypothenar muscle group was removed along with any remaining flexor retinaculum to fully expose the transverse carpal ligament. The contents of the carpal tunnel were left intact along with the tendons for flexor carpi ulnaris and flexor carpi radialis.

Sample specimen dissection images can be found in Appendix C.

3.4.2 Specimen Mounting

Following preparation, the specimens were secured to a flat aluminium platform attached to the lower crosshead of the testing machine. The specimens were secured to the platform, supinely and in a neutral wrist posture, by three aluminium bars: one distal across the heads of the 2nd – 5th metacarpals and the 1st distal interphalangeal joint (thumb); and two proximal, across the distal forearm. The specimens were fully secured once centrally located below the indenter. The lower crosshead platform was then raised to position the specimen in as close proximity as possible, without contact, to the indenter.

3.4.3 Test Protocol

The test protocol was developed using the Wintest 4.1 software package and one pilot cadaveric hand specimen.

The actuator of the BOSE testing machine has an operational displacement range of ± 6.50 mm (13.00 mm total range). Safety displacement limits were set to ± 5.50 mm and load safety limits were set to ± 400.00 N in order to protect the load cell from damage. A peak displacement of 8.00 mm was originally chosen, in line with the protocol described in a similar study by Chaise *et al* (2003), for the test protocol; however, this displacement could not be achieved without failing the 400.00 N safety

limit of the load cell. A peak displacement of 4.50 mm was found to be the largest safe displacement that left a suitable margin for specimen peak load variability.

Stage 1: Preconditioning cycle

The indenter was lowered to 0.50 N preload contact with the specimen. Current displacement was recorded and a peak displacement -4.50 mm from this position was calculated and entered into the software package. Ten sine wave preconditioning cycles of 4.50 mm displacement at a rate of 2 Hz were performed. A half sine block was added to ensure the indenter finished the tenth cycle at 0.00 mm relative displacement.

Stage 2: Recovery

A short recovery period of 10 s was then afforded the specimen following the precondition cycle.

Stage 3: Displacement Ramp and Hold

Following the 10 s recovery period, a ramped displacement of -4.50 mm at 2.00 mm/s was performed and held at constant displacement (constant strain) for 1800 s (30 minutes).

A 1 hour recovery period followed completion of the test; the specimen was removed from the platform and dissected in preparation the next trial. During the recovery period hydration of the specimens was maintained using a 0.9% phosphate buffered saline solution (1 tablet per 200 ml water) sprayed onto the specimens following dissection.

3.5 Data Analysis

Time (s), load (N) and displacement (mm) data was sampled at a frequency of 200 Hz and 1 Hz for the ramped displacement and load relaxation (hold) portions of the test respectively. A higher sampling frequency for the ramped displacement was

chosen to more accurately calculate stiffness of the tissue. Stiffness was calculated as the slope of the linear portion of the stress/strain graph and a minimum linear regression (R^2 -value) was set at $R^2 = 0.95$ for all trials (Holmes *et al*, 2011).

3.5.1 Calculation of Ligament Strain

Ligament elongation and strain was calculated using a method developed by Holmes *et al* (2011). Figure 1, below illustrates a simple 2D model of a cross section of the mid TCL-carpal arch; used to calculate the final ligament length.

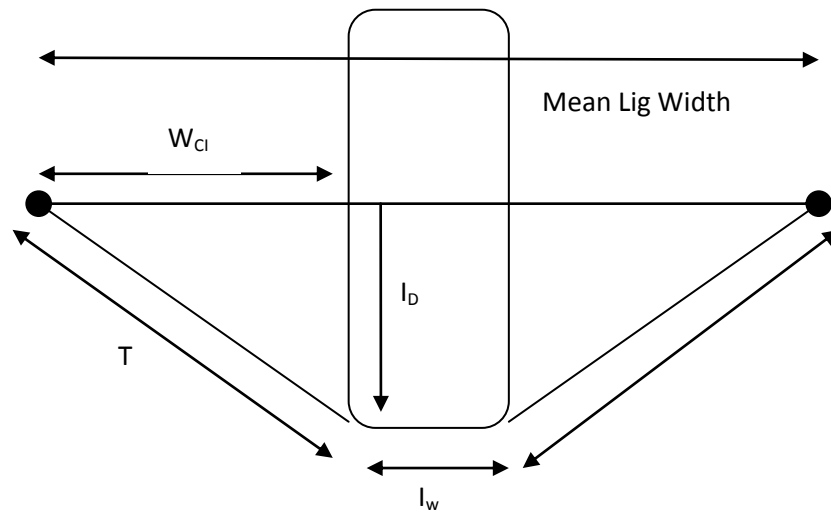


Figure 3: Simple 2D model of final ligament width: final ligament length is calculated from Pythagoras Theorem. Where: W_{CI} = half ligament width – half indenter width; I_D = Indentation depth; and I_w = Indenter width.

Proximal, mid, and distal ligament width were recorded for all specimens. The mean of these three widths was used for this calculation. Ligament width during indentation can be calculated as

$$L_w = (2 \times T) + I_w \quad (1)$$

Where L_w = instantaneous ligament width, T = length of TCL on either side of the Indenter, and I_w = indenter width.

3.6 Statistical Analysis

Paired t-tests were used to compare the difference in means between conditions (dissection level); within subjects, and unpaired t-tests were used to compare the difference in mean scores, between subjects, for comparison between the ‘Hypothenar Removed’ and ‘Thenar Removed’ conditions.

For all comparisons, alpha (α) was set at 0.05.

Validity for performing these parametric statistical tests are inferred from tests performed for assumption of parametric use.

Measures of central tendency are reported via means and standard deviations ($M \pm SD$) and the statistical results of the t-tests are reported with regards to the means, standard error, t-value (with degrees of freedom), significance value (p), and the power of the significance (r-value) of the two conditions being compared.

4 Results

Tests were completed for the assumption of the use of a parametric inferential test. The three measured dependent variables (Peak Load (N), Stiffness (N/mm), and 80% Relaxation Time (s)) are all ratio level data.

Specimens were chosen at random from a selection of cadaveric hands available at the Laboratory of Human Anatomy, University of Glasgow, Scotland.

All data sets (except for Relaxation Time: Thenar Group: Intact* and TCL Exposed**) are normally distributed (Table 3). Tests of normality were performed using Anderson-Darling test for normality since degrees of freedom is less than 50 (df = 2 to 5). All graphical representations for normal distribution of the data can be found in Appendix D.

Table 1: Anderson-Darling test for Normality (* unable to perform normality due to degrees of freedom = 1, ** contains an outlier)

		Intact	Skin Removed	Thenar Removed	Hypothenar Removed	TCL Exposed
Load	Hypothenar Group	$P = 0.294$	$P = 0.239$		$P = 0.096$	$P = 0.535$
	Thenar Group	$P = 0.146$	$P = 0.519$	$P = 0.229$		$P = 0.080$
	Combined	$P = 0.167$	$P = 0.142$			$P = 0.690$
Stiffness	Hypothenar Group	$P = 0.454$	$P = 0.565$		$P = 0.526$	$P = 0.248$
	Thenar Group	$P = 0.079$	$P = 0.142$	$P = 0.181$		$P = 0.570$
	Combined	$P = 0.246$	$P = 0.259$			$P = 0.209$
Relaxation Time	Hypothenar Group	$P = 0.527$	$P = 0.304$		$P = 0.292$	$P = 0.503$
	Thenar Group	*	$P = 0.630$	$P = 0.087$		$P = 0.118$
	Combined	$P = 0.072$	$P = 0.279$			$P = <0.005$ **

Homogeneity of variance was tested for using Bartlett's Test. Equal Variance can be assumed for all data (graphs for homogeneity of variance with Bonferroni 95% Confidence Intervals can be found in Appendix E).

Table 2: Bartlett's Test for equal variance

	Test Statistic	Sig.
Peak Load	18.04	<i>P</i> = 0.054
Stiffness	8.12	<i>P</i> = 0.617
Relaxation Time	12.35	<i>P</i> = 0.262

4.1 Load Relaxation

Peak load corresponds to the load recorded at the end of the displacement ramp, or beginning (0 s) of the load relaxation. The mean time (seconds) for the load to drop to 80% of peak load for each group's condition is also reported (** Includes possible outlier, excluding = 210 ± 99 s).

Table 3: Mean \pm SD Peak Loads and Load relaxation results for the three test groups across all conditions

		Peak Load (N)	1 s	10 s	100 s	1000 s	Min Load (1800 s)	80% Load Relaxation Time
<i>Hypothenar Group</i>	Intact	76.11 \pm 40.21	60.08 \pm 31.90	36.59 \pm 18.83	19.03 \pm 9.99	10.20 \pm 5.86	8.98 \pm 5.36	293 \pm 171
	Skin Removed	115.48 \pm 75.39	93.93 \pm 67.60	52.58 \pm 36.43	24.64 \pm 14.43	13.44 \pm 6.88	12.11 \pm 6.06	146 \pm 54
	Hypothenar Removed	115.71 \pm 64.9	94.98 \pm 60.83	54.13 \pm 35.64	24.70 \pm 16.28	13.09 \pm 8.66	11.78 \pm 7.79	123 \pm 60
	TCL Exposed	172.51 \pm 75.39	148.21 \pm 71.35	85.52 \pm 37.58	39.01 \pm 16.70	19.05 \pm 8.63	16.71 \pm 7.55	147 \pm 19
<i>Thenar Group</i>	Intact	59.93 \pm 52.74	43.53 \pm 34.62	29.30 \pm 21.94	17.11 \pm 11.67	9.33 \pm 5.97	8.01 \pm 5.14	422 \pm 5
	Skin Removed	128.10 \pm 67.40	109.72 \pm 64.51	65.60 \pm 39.48	31.62 \pm 18.49	15.54 \pm 8.83	13.50 \pm 7.71	223 \pm 115
	Thenar Removed	228.15 \pm 101.18	209.73 \pm 113.42	122.43 \pm 69.66	59.09 \pm 37.26	29.44 \pm 19.00	25.64 \pm 16.56	206 \pm 125
	TCL Exposed	186.77 \pm 47.32	173.88 \pm 50.30	115.16 \pm 35.75	63.13 \pm 23.87	32.12 \pm 14.30	27.75 \pm 12.72	715 \pm 670
<i>Combined Group</i>	Intact	68.02 \pm 42.87	51.81 \pm 31.12	32.95 \pm 18.72	18.07 \pm 9.77	9.77 \pm 5.31	8.50 \pm 4.73	344 \pm 140
	Skin Removed	121.79 \pm 64.33	101.83 \pm 59.73	59.09 \pm 34.71	28.13 \pm 15.32	14.49 \pm 7.17	12.81 \pm 6.25	154 \pm 91
	TCL Exposed	179.64 \pm 56.84	161.05 \pm 56.98	100.34 \pm 36.60	51.07 \pm 22.67	25.59 \pm 12.76	22.23 \pm 11.14	440 \pm 587**
TCL Only		19.80	17.44	13.82	9.9	7.02	6.52	67.07%

Normalised load relaxations with time for the three groups are illustrated in figures 2 to 4, below. The rapid load relaxation within the first 100 seconds is evident across all groups followed by a more gradual relaxation to 1000 s.

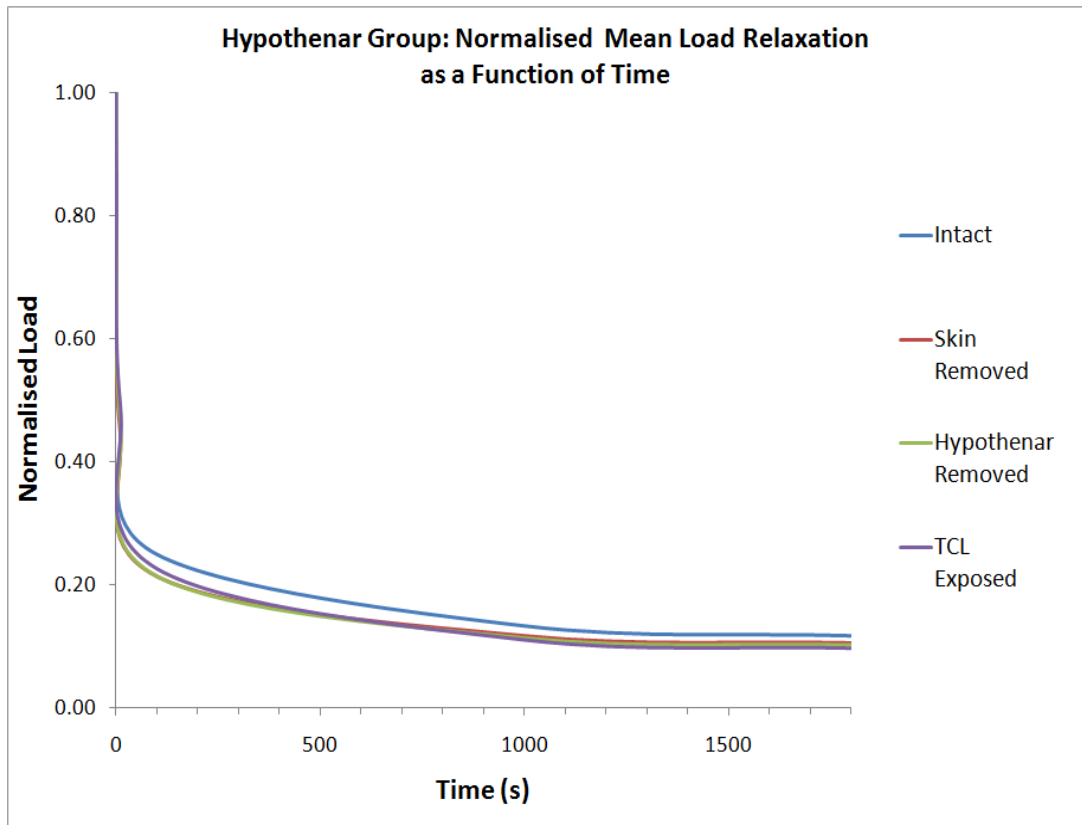


Figure 4: Normalised mean load relaxation graph for the Hypothenar Group; illustrating the similar viscoelastic properties at the different levels of dissection.

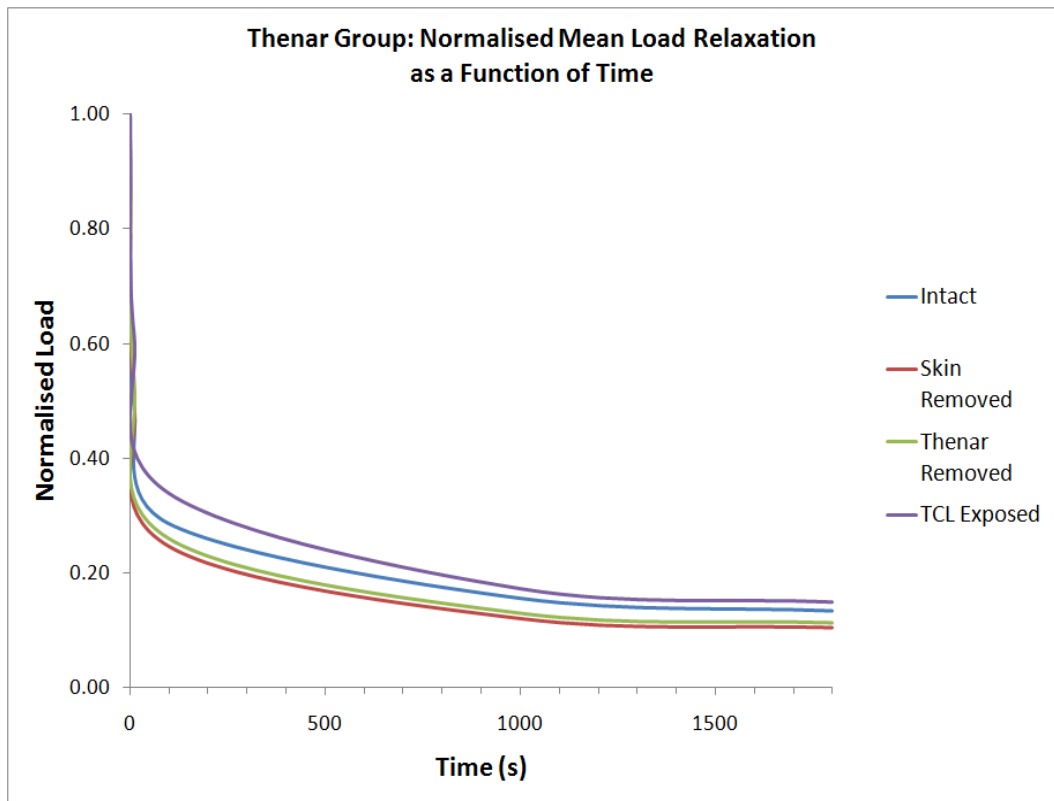


Figure 5: Normalised mean load relaxation graph for the Thenar Group.

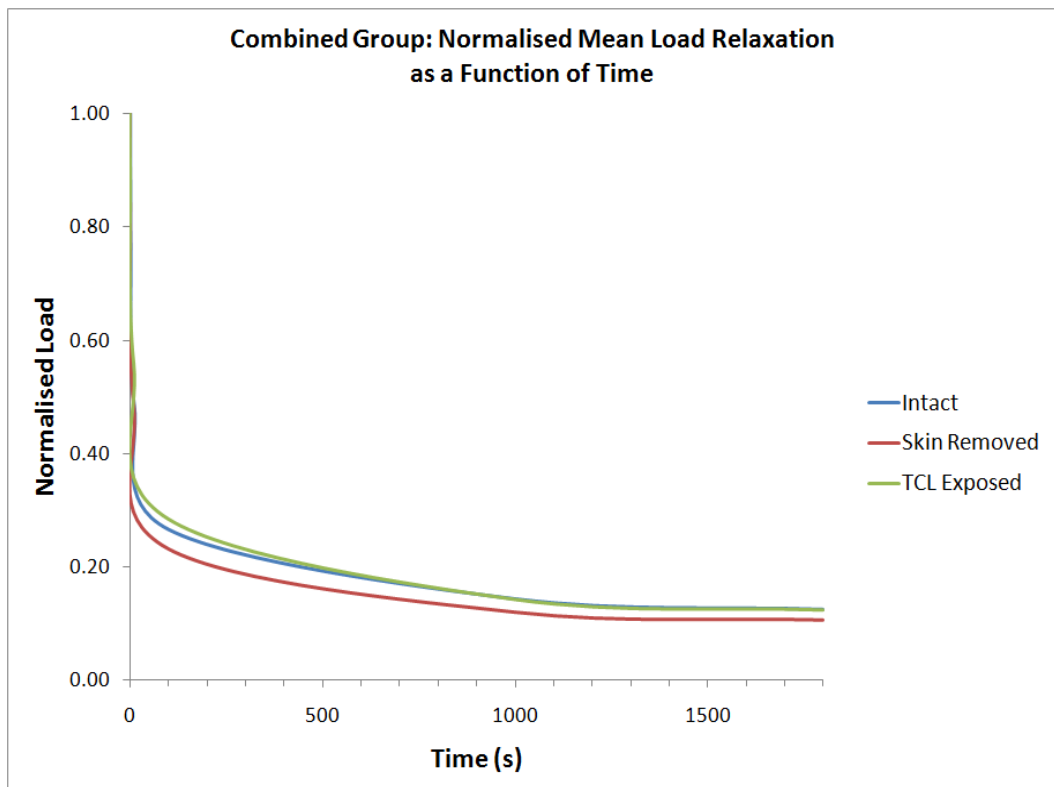


Figure 6: Normalised mean load relaxation for the Combined Group.

Paired t-tests were performed to compare the difference in means between the different levels of dissection within each group. All six specimens were tested at the 'Intact', 'Skin Removed' and 'TCL Exposed' levels. Following indentation at the 'Skin removed' level, three specimens underwent dissection to remove the Hypothenar muscle group first (leaving the Thenar muscle group intact) while the other three specimens had the Thenar muscle group removed first (leaving the Hypothenar muscle group intact).

4.1.1 Combined Group:

The time taken to reach 80% load relaxation was significantly longer for the 'Intact' hands ($M = 344$, $SE = 63$) compared to the 'Skin Removed' condition ($M = 154$, $SE = 26$), $t(9) = 3.19$, $p = 0.033$, $r = .73$. There were no other significant differences found for relaxation time for any group though some differences were observed. The 'TCL Exposed' condition took slightly longer to relax ($M=440$, $SE=263$) than the 'Intact' condition ($M=344$, $SE=63$) and the 'Skin Removed' condition ($M=154$, $SE=26$).

4.1.2 Hypothenar Group:

'Intact' ($M=293$, $SE=99$) relaxation time was longer than 'Hypothenar Removed' ($M=123$, $SE=34.8$), $t(4)=1.38$, $p=0.303$, $r=.57$. No difference in relaxation time was noted between 'Skin Removed' and 'Hypothenar Removed', and between 'Hypothenar Removed' and 'TCL Exposed'.

4.1.3 Thenar Group:

Two large but non-significant differences were noted in the Thenar Group. 'Intact' ($M=422$, $SE=3.5$) relaxation time was longer than 'Thenar Removed' ($M=206$,

SE=72) and ‘TCL Exposed’ (M=715, SE=387) relaxation time was greater than ‘Thenar Removed’ (M=206, SE=72).

4.1.4 Between Group:

The ‘Hypothenar Removed’ condition (M=123 s, SE=35) showed faster load relaxation than the ‘Thenar Removed’ condition (M=206 s, SE=72), $t(4)=-1.04$, $p=0.409$, $r=0.46$, though not significantly slower.

Table 4: t-test results for Relaxation Time (s) (M = Mean, SE = Standard Error) (* = Significant difference).

	Condition 1	Condition 2	M (Condition 1)	SE (Condition 1)	M (Condition 2)	SE (Condition 2)	t(df)	t- Value	P- Value	r
Combined Group	Intact	Skin Removed	344	63	154	26	9	3.19	0.033*	0.73
	Intact	TCL Exposed	344	63	440	263	9	-0.39	0.719	0.13
	Skin Removed	TCL Exposed	154	26	440	263	10	-1.20	0.283	0.35
Hypothenar Group	Intact	Hypothenar Removed	293	99	123	35	4	1.38	0.303	0.57
	Skin Removed	Hypothenar Removed	146	31	123	35	4	0.70	0.556	0.33
	Hypothenar Removed	TCL Exposed	123	35	147	11	4	-0.94	0.446	0.43
Thenar Group	Intact	Thenar Removed	422	4	206	72	3	1.70	0.339	0.70
	Skin Removed	Thenar Removed	223	66	206	72	4	0.18	0.874	0.09
	Thenar Removed	TCL Exposed	206	72	715	387	4	-1.61	0.248	0.63
Between Group Comparison										
	Hypothenar Removed	Thenar Removed	123	35	206	72	4	-1.04	0.409	0.46

4.2 Peak Load

4.2.1 Combined Group:

The peak load following 4.5 mm indentation was recorded and compared between the dissection levels (conditions) for the three groups. The peak load on the 'Intact hands' (M=68.0 N, SE=17.5) was significantly lower than that experienced for the 'TCL Exposed' condition (M=179.6 N, SE=23.2), $t(10)=-3.78$, $p=0.013$, $r=.77$, and 'Intact' was also lower, but not significantly, than the 'Skin Removed' condition (M=121.8 N, SE=26.3), $t(10)=-2.49$, $p=0.055$, $r=.62$.

4.2.2 Hypothenar Group:

Within the Hypothenar group the 'TCL Exposed' condition recorded the highest mean load (M=172.5 ± 75.39 N, SE=43.5) though this load was not significantly greater than the 'Hypothenar Removed' condition (M=115.7 N, SE=37.5), $t(4)=-3.05$, $p=0.093$, $r=.84$.

No mean difference in load was noted between 'Skin Removed' (M=115.5 N, SE=43.5) condition and the 'Hypothenar Removed' condition (M=115.7 N, SE=37.5), $t(4)=-0.03$, $p=0.980$, $r=.01$.

4.2.3 Thenar Group:

The 'Thenar Removed' condition (M=228.2 N, SE=58.4) recorded a significantly greater peak load than both the 'Intact' condition (M=59.9 N, SE=30.4), $t(4)=-5.99$, $p=0.027$, $r=.95$, and the 'Skin Removed' condition (M=128.1 N, SE=38.9), $t(4)=-4.67$, $p=0.043$, $r=0.92$. The 'Thenar Removed' condition also recorded a higher mean peak load than the 'TCL Exposed' condition (M=186.8 N, SE=27.3), $t(4)=0.73$, $p=0.540$, $r=0.34$ though this difference is not significant.

4.2.4 Between group:

The ‘Hypothenar Removed’ condition (M=115.7 N, SE=37.5) reported a lower peak load than the ‘Thenar Removed’ condition (M=228.2 N, SE=58.4), $t(4)=-1.62$, $p=0.204$, $r=0.63$, though not significantly lower.

Table 5: Paired t-test results for Peak Load (* Significant difference)

	Condition 1	Condition 2	M (Condition 1)	SE (Condition 1)	M (Condition 2)	SE (Condition 2)	t(df)	t- Value	P- Value	r
Combined Group	Intact	Skin Removed	68.0	17.5	121.8	26.3	10	-2.49	0.055	0.62
	Intact	TCL Exposed	68.0	17.5	179.6	23.2	10	-3.78	0.013*	0.77
	Skin Removed	TCL Exposed	121.8	26.3	179.6	23.5	10	-2.54	0.052	0.63
Hypothenar Group	Intact	Hypothenar Removed	76.1	23.2	115.7	37.5	4	-1.09	0.390	0.48
	Skin Removed	Hypothenar Removed	115.5	43.5	115.7	37.5	4	-0.03	0.980	0.01
	Hypothenar Removed	TCL Exposed	115.7	37.5	172.5	43.5	4	-3.05	0.093	0.84
Thenar Group	Intact	Thenar Removed	59.9	30.4	228.2	58.4	4	-5.99	0.027*	0.95
	Skin Removed	Thenar Removed	128.1	38.9	228.2	58.4	4	-4.67	0.043*	0.92
	Thenar Removed	TCL Exposed	228.2	58.4	186.8	27.3	4	0.73	0.540	0.34
Between Group Comparison										
	Hypothenar Removed	Thenar Removed	115.7	37.5	228.2	58.4	4	-1.62	0.204	0.63

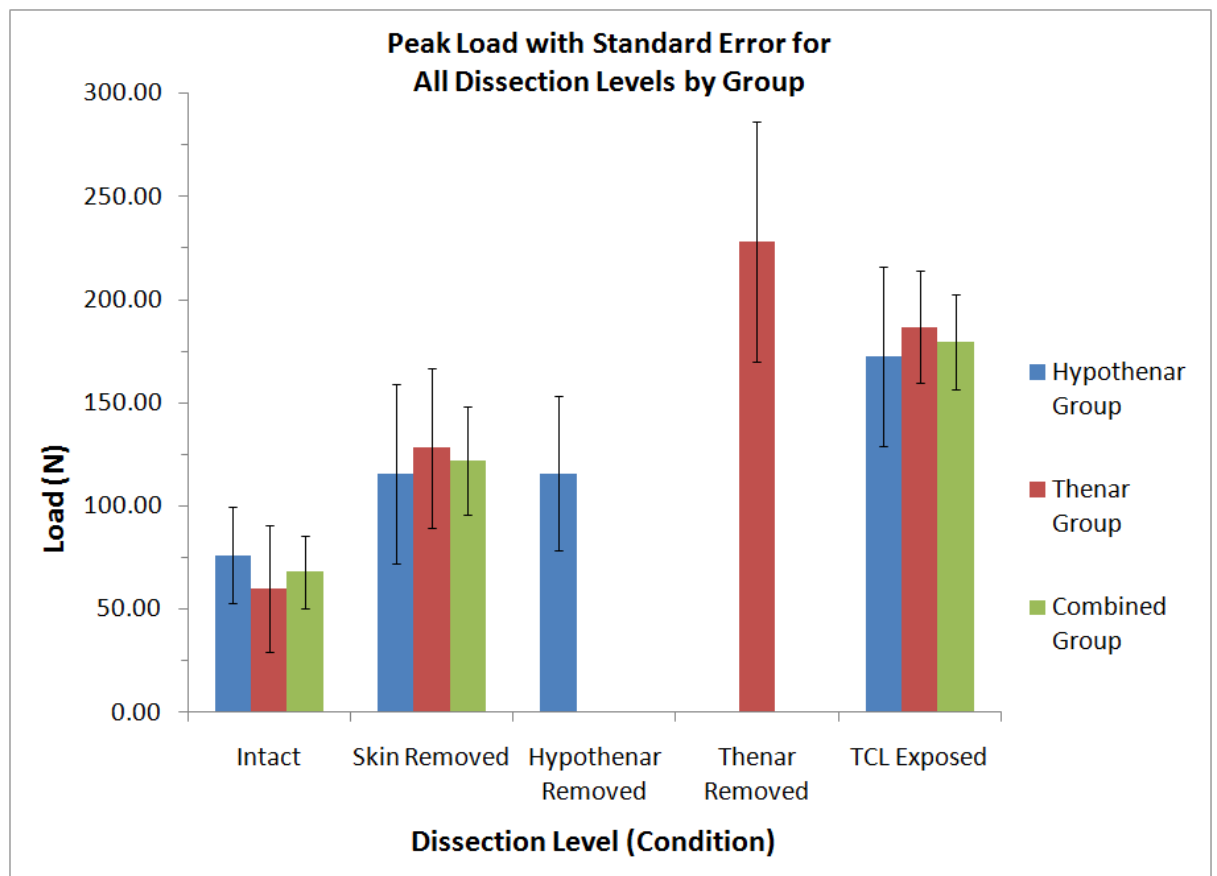


Figure 7: Mean Peak loads and standard error for all dissection levels and groups. Illustrates the general increase in peak loads with each level of dissection.

Figure 5 above illustrates the increase in load peak load recorded with individual standard errors. Peak load can be seen to increase after each dissection with the exception of the ‘Hypothenar Removed’ level of dissection, which does not show any increase in peak load recorded over the ‘Skin Removed’ condition.

4.3 Stiffness

4.3.1 Combined Group:

Within the combined group, the ‘TCL Exposed’ condition (M=27.05 N/mm, SE=4.94) recorded the greatest stiffness; being significantly higher than the ‘Intact’ condition (M=8.50 N/mm, SE=2.52), $t(10)=-3.12$, $p=0.026$, $r=.70$, and greater but not significantly, than the ‘Skin Removed’ condition (M=16.90 N/mm, SE=3.50), $t(10)=-2.25$, $p=0.074$, $r=.58$.

4.3.2 Hypothenar Group:

No significant difference were observed within the Hypothenar group, though ‘TCL Exposed’ showed slightly greater stiffness (M=20.96 N/mm, SE=2.94) than the ‘Hypothenar Removed’ condition (M=14.19 N/mm, SE=3.01), $t(4)=-4.12$, $p=0.054$, $r=.90$. No difference in stiffness was noted between ‘Skin Removed’ (M=13.24 N/mm, SE=3.68) and the ‘Hypothenar Removed’ condition $t(4)=-0.85$, $p=0.485$, $r=0.39$.

4.3.3 Thenar Group:

A large but not significant difference was found between the stiffness of the ‘Intact’ condition (M=7.17 N/mm, SE=2.9) and that of the ‘Thenar Removed’ condition (M=30.73 N/mm, SE=9.92), $t(4)=-3.35$, $p=0.079$, $r=.86$. The stiffness for the ‘Skin Removed’ condition (M=20.57 N/mm, SE=5.85) was approximately 33% lower than that for the ‘Thenar Removed’ condition (M=30.73 N/mm, SE=9.92), $t(4)=-2.26$, $p=0.152$, $r=.75$, and ‘Thenar Removed’ was only slightly less stiff than ‘TCL Exposed’ (M=33.14 N/mm, SE=8.75), $t(4)=-0.18$, $p=0.874$, $r=.09$.

4.3.4 Between Groups:

Stiffness was greater for the ‘Thenar Removed’ condition (M=30.7 N/mm, SE=9.9) compared to the ‘Hypothenar Removed’ condition (M=14.19 N/mm, SE=3.0), $t(4)=-1.60$, $p=0.251$, $r=0.62$, though the difference is not significant.

Table 6: Paired t-test results and significance* values for stiffness

	Condition 1	Condition 2	M (Condition 1)	SE (Condition 1)	M (Condition 2)	SE (Condition 2)	t(df)	t- Value	P- Value	r
Combined Group	Intact	Skin Removed	8.50	2.52	16.90	3.50	10	-2.54	0.052	0.63
	Intact	TCL Exposed	8.50	2.52	27.05	4.94	10	-3.12	0.026*	0.70
	Skin Removed	TCL Exposed	16.90	3.50	27.05	4.94	10	-2.25	0.074	0.58
Hypothenar Group	Intact	Hypothenar Removed	9.82	4.66	14.19	3.01	4	-0.85	0.483	0.39
	Skin Removed	Hypothenar Removed	13.24	3.68	14.19	3.01	4	-0.85	0.484	0.39
	Hypothenar Removed	TCL Exposed	14.19	3.01	20.96	2.94	4	-4.12	0.054	0.90
Thenar Group	Intact	Thenar Removed	7.17	2.90	30.73	9.92	4	-3.35	0.079	0.86
	Skin Removed	Thenar Removed	20.57	5.85	30.73	9.92	4	-2.26	0.152	0.75
	Thenar Removed	TCL Exposed	30.73	9.92	33.14	8.75	4	-0.18	0.874	0.09
Between Group Comparison										
	Hypothenar Removed	Thenar Removed	14.19	3.0	30.7	9.9	2	-1.60	0.251	0.62

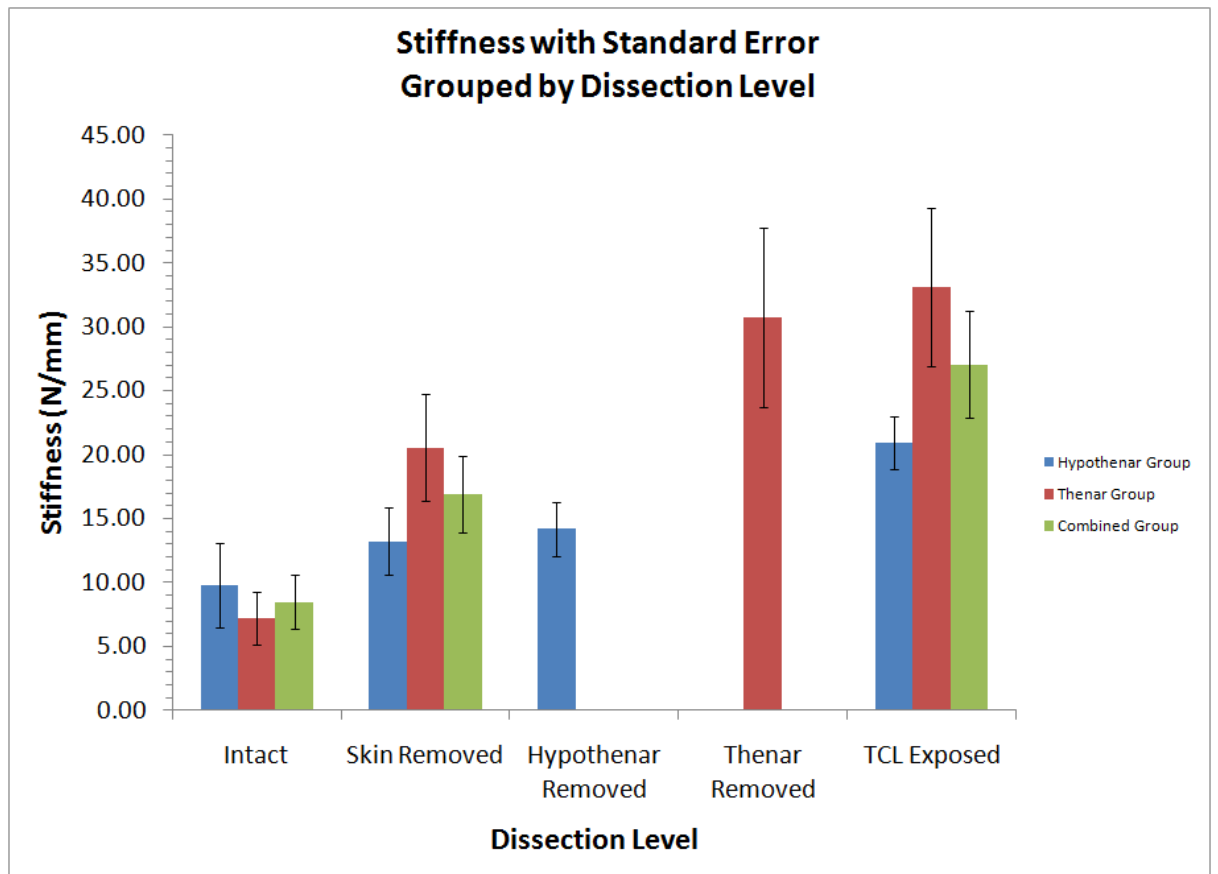


Figure 8: Mean stiffness with standard error across all dissection levels an groups. This graph illustrates the general increase in recorded stiffness at each subsequent level of dissection.

As with peak load, the stiffness can be seen to increase with each level of additional dissection, again with the exception of the removal of the hypothenar muscles which showed no increase in stiffness compared to the ‘Skin Removed’ level of dissection.

Anthropometric measurements for all specimens can be found in Appendix F.

5 Discussion

The purpose of this investigation was to examine the viscoelastic and mechanical properties of the transverse carpal ligament and to quantitatively describe the contribution of the soft tissue layers superficial to the TCL.

Peak load differences were large among the three conditions of the combined group with subsequent levels of dissection resulting in an increase in peak loads (68.02 ± 42.87 , 121.79 ± 64.33 and 179.64 ± 56.84 N for Intact, Skin removed, and TCL exposed conditions respectively) however the only significant difference found was between 'Intact' and 'TCL Exposed' conditions ($t(10)=-3.78$, $p=0.013$, $r=.77$). The general increase in peak loads observed gives an indication of the load absorption capability of each layer of tissue. The 'Intact' hand reported a mean of 111.62 N less than 'TCL exposed' while the 'Skin removed' condition resulted in 57.85 N less than 'TCL exposed' and 53.77 N more than 'Intact'. From this we can say that the skin and adipose layer provided an average of 53.77 N of load absorption and the combined hypothenar/thenar layer provided an average of 57.85 N of load absorption.

Within the thenar group, the highest peak load recorded was by the 'Thenar removed' condition (228.15 ± 101.18 N) which was significantly greater than both the 'Intact' and 'Skin removed' conditions, and higher (but not significantly) than the 'TCL exposed' condition.

The hypothenar group showed a different trend with the 'Hypothenar removed' condition reporting the same mean peak load as the 'Skin removed' condition (115.71 ± 64.9 N and 115.48 ± 75.39 N respectively).

A large amount of load relaxation occurred across all conditions and groups, reaching 45-61% relaxation within the first 10 s. The time taken to reach 80% relaxation occurred for all conditions (except 'TCL exposed' of the thenar group) within 123 s to 440 s, with an average of 253 s.

The only significant difference to occur between conditions was among the combined group; 'Intact' ($M = 344$ s, $SE = 63$) took significantly longer than 'Skin removed' ($M = 154$ s, $SE = 26$) to reach 80% load relaxation. Another notable pattern across all groups was that the 'Intact' condition always took longer to reach

80% relaxation than any other condition. It should be noted that within the ‘TCL exposed’ condition of the thenar group, one specimen recorded an 80% relaxation time of 1486 s; exceptionally longer than any other specimen across all conditions. With the removal of this outlier the mean \pm SD 80% relaxation time is 329 ± 79 s and 210 ± 99 s for the ‘TCL exposed’ conditions of the thenar and combined groups respectively.

Across all groups, stiffness generally increased as tissue layers were dissected away. The only significant change however, was within the combined group for ‘Intact’ vs. ‘TCL exposed’ (8.50 ± 6.18 N/mm and 27.05 ± 12.11 N/mm respectively).

Non-significant differences were found between ‘hypothenar removed’ and ‘thenar’ removed’ for all of the dependant variables. Removal of the thenar muscles resulted in longer 80% relaxation times (67.5% longer), and greater peak loads (97.2% greater) and stiffness (116.6% greater) compared to the removal of the hypothenar muscles.

No statistical analysis was done for the ‘TCL only’ condition as only one specimen was tested in this condition.

5.1 Peak Load and Load Relaxation

The peak loads recorded in this investigation are consistently greater than those reported by Chaise *et al* (2003). Test methodologies between the two studies are very similar and so some comparisons can be made. The mean peak loads recorded for the ‘Intact’ and ‘TCL exposed’ conditions in this study were 68.02 ± 42.87 N and 179.64 ± 56.84 N respectively, compared to 27.1 N and 80.5 N respectively reported by Chaise *et al* (2003). Though our recorded peak loads may be higher, the percentage increase in loads between the two conditions for both studies is very similar (62% and 66.3 % increases in peak load for the ‘TCL exposed’ conditions of our study and that for Chaise *et al*, 2003, respectively). A possible explanation for the greater peak loads in our study may be our use of embalmed specimens as opposed to the fresh frozen specimen used by Chaise *et al* (2003). Formalin fixation has been reported in the literature to alter the mechanical properties of biological tissue through the formation of additional intramolecular and intermolecular cross-

links in proteins (Wilke *et al*, 1996), thus adding rigidity to the tissue. Wilke *et al* (1996) found formalin fixed bovine functional spine units to display an 80% reduction in range of motion (ROM) and greater stiffness compared to pre-fixation ROM (fresh). Viidik and Lewin (1966) found formaldehyde fixed rabbit knee ligaments demonstrated greater stiffness, lower failure loads and less elongation compared to a control group. Both authors conclude that fixed tissue mechanics are not entirely representative of those for fresh tissue. The choice to use embalmed specimens for this study is further discussed in the limitations of the study.

Load relaxation appears to be greater for our study compared to those reported by Chaise *et al* (2003). The mean time to reach 80% load relaxation for the 'Intact' condition in our study was 344 ± 140 s and by 1000s the load had relaxed to only 14.4% of peak load. Chaise *et al* (2003) reports that the load on the palmar surface took 20-30 minutes (1200-1800 s) to reach an equilibrium load of 23.5%. For the 'TCL exposed' condition, relaxation was greater than the 'Intact' conditions for both our study and that of Chaise *et al* (2003). In our study, 80% relaxation was reached in 210 ± 99 s and reached 85.8% by 1000 s; while Chaise *et al* (2003) reports 83.2% relaxation was reached between 20 and 30 minutes. The greater load relaxation reported in our study may be due to the lower strain level imposed. A displacement of 4.5 mm was used here compared to 8.0 mm used by Chaise *et al* (2003). These results support the findings of others (Van Loocke *et al*, 2008 and Bonifasi-Lista *et al*, 2005) in that the rate of relaxation is greater for smaller levels of strain. Some care must be taken though in making these comparisons as the results reported by Chaise *et al* (2003) are based on one fresh frozen specimen and this may not be entirely representative of the normal population.

5.1.1 Tissue layer differences

As stated previously, the peak load increased with each dissection level and this may give an indication of the load absorption capability of each layer of tissue above the TCL. With regards to the results for the Combined Group, the 'intact' condition

recorded a peak load of 68.02 ± 42.87 N which is 53.77 N lower than 'skin removed' (121.79 ± 64.33 N) and 111.62 N lower than 'TCL exposed' (179.64 ± 56.84 N), while 'skin removed' was 57.85 N lower than 'TCL exposed'. The layers of the skin and the subcutaneous adipose provided a large amount of load absorption (though not significant different) while the combined soft tissue layers provided a significantly large amount of load absorption ('Intact' vs. 'TCL exposed'). It is to be expected that as tissue thickness increases the load dissipation would also increase (Smalls *et al*, 2006). A large proportion of the load recorded on the 'Intact' hand can be possibly attributed to the layers of the dermis and epidermis. Miller-Young *et al* (2002) found peak stresses on human calcaneal fat pads of 21.3 kPa (0.0213 N/mm²) when 10 mm thick by 8 mm diameters fat pad sections were compressed to 40% strain. In comparison, a peak stress of 866 kPa (0.866 N/mm²) was calculated for the 'Intact' condition in this study (based on a load of 68.02 N divided by indenter area of 78.54 mm²). The larger stresses recorded in our study may be attributed to the skin layer over the subcutaneous adipose tissue. Miller-Young *et al* (2002) found the calcaneal fat pad samples to stress relax very rapidly, attributing it to the high unsaturated fatty acid ratio of the fat pads found in load bearing areas.

The effect on recorded peak load due to removing of one of the muscle groups is of particular interest. Within the Hypothenar Group, there was no difference in peak loads between the 'Skin removed' (115.48 ± 75.39 N) and 'Hypothenar removed' (115.71 ± 64.90 N). While within the Thenar Group, the peak loads for 'Skin removed' (128.10 ± 67.40 N) was significantly less than 'Thenar removed' (228.15 ± 101.18 N). This indicating that the thenar muscle group's attachment onto the TCL absorbs far more load than the hypothenar attachment. Though not recorded objectively, visual inspection of the specimens during dissection did reveal that the thenar attachment on the TCL was visibly thicker and covered a greater area of the ligament compared to the hypothenar attachment. Unfortunately these parameters were not recorded and this is an obvious limitation to this study.

Another notable difference (though not significantly) was the longer 80% relaxation times for the 'Intact' conditions compared to all other conditions and across groups. For the Combined Group, the 'Intact' condition (344 ± 140 s) took 123.3% longer to

reach 80% relaxation than the 'Skin removed' condition (154 ± 91 s) and 63.8% longer than 'TCL exposed' (210 ± 99 s (outlier removed value)). Within the Hypothenar Group, the 'Intact' condition (293 ± 171 s) took 138.2% longer to reach 80% relaxation compared to 'Hypothenar removed' (123 ± 60 s), while in the Thenar Group, the 'Intact' condition (422 ± 5 s) took approximately twice as long as the 'Thenar removed' condition (206 ± 125 s). A possible explanation for this may be the effect of the skin layer causing the longer relaxation times. Crichton *et al* (2011) found that the stratum corneum and dermal layer of mouse skin reached a plateau at about 40% relaxation. The author posited that this maybe due to the lower hydration level ($\sim 15\%$) and stiffer nature of the stratum corneum compared to the deeper layers. As mentioned earlier; the variability in specimen quality and use of embalmed specimens in this study should be considered when interpreting the results. There was a notable variation in the level of embalming fluid content among the specimens tested in this study; presenting difficulties in controlling for moisture across the specimens.

5.2 Stiffness

The stiffness of the 'Intact' condition (8.5 ± 6.2 N/mm) in the current study is similar to that reported in the literature. Chaise *et al* (2003) reports palmar surface stiffness values of 15.6, 8.2, and 6.8 N/mm for 1st, 2nd and 3rd trials respectively. The author discusses only the 2nd trial values as they are closer to those of the 3rd trial, surmising that the large decrease from the 1st trial scores are due to preconditioning. However, the author also reports that preconditioning cycles were included at the start of all trials. For this reason, the values from the first trial will also be considered here. Zheng *et al* (2006) reported stiffness values for tissue covering the TCL of 3.57 N/mm and 18.98 N/mm when indenting with 0-5 N and 5-20 N loads respectively, and reporting a mean value of 6.72 ± 2.10 N/mm. These values are comparable to those in the current study despite lower indentation loads being applied with an ultrasound probe and to live human tissue also.

At the 'TCL exposed' level, a stiffness 3.2 times greater (27.05 ± 12.11 N/mm) than at the 'Intact' level was recorded in the current study. Again, this is comparable to those reported elsewhere. Chaise *et al* (2003) reported a stiffness values 3 to 3.6 times greater for their TCL-exposed condition (29.8 to 46.0 N/mm). Zheng *et al* (2006) recorded stiffness values for the tissue layer between the TCL and floor of the carpal tunnel of up to 21.76 N/mm, while Holmes *et al* (2011) report a stiffness value of 35.9 ± 2.8 N/mm for their TCL exposed condition. These values can be considered comparable if consideration is given to the range of the individual scores for the current study (17.11 to 47.23 N/mm). The relatively high variation in stiffness values among the specimens is most likely attributable to variability in interspecimen quality and condition, and to the relatively small sample size. (n=6).

5.2.1 Tissue Layer Differences

Across all groups stiffness generally increased as tissue layers were dissected away. The differences though are not significant with the exception of ‘Intact’ vs. ‘TCL exposed’ for the Combined Group. A similar pattern was found for stiffness values between the layers as was seen for the peak load values.

Within the Hypothenar Group, the removal of the hypothenar muscle group had no effect on the stiffness recorded (‘Hypothenar removed’: 14.19 ± 5.21 N/mm; ‘Skin removed’: 13.24 ± 6.38 N/mm), while in the Thenar Group, removal of the thenar muscle group resulted in a 49.4% increase in stiffness compared to ‘Skin removed’ (‘Thenar removed’: 30.73 ± 17.17 N/mm; ‘Skin removed’: 20.57 ± 10.13 N/mm).

Again, the reason for this difference may be due to the extent to which the muscle fibres of the thenar eminence traverse the TCL and the thickness of this insertion layer. The viscoelastic properties of a layer of muscle fascicles above the TCL are likely to dissipate energy and result in a lower recorded value for stiffness.

However, it is important to consider the orientation of the muscle fibres in relation to the compressive force. In the current study, indentation is perpendicular to the palmar surface. Therefore, the compression of the muscle fibres of the thenar muscle group will be in a cross-fibre direction and, as such, stiffness should be reported for cross-fibre direction and not axial tensile stiffness (Van Looke *et al* 2008). Greater stiffness may be observed in a cross-fibre direction compared to with-fibre direction when strain rates are low ($<5\% \text{ s}^{-2}$) as was the case in this study (average of $4.2\% \text{ s}^{-1}$).

An important consideration when analysing the results of the tissue properties on the exposed TCL is the effect of tissues in the carpal tunnel and carpal arch itself.

Indentation of the exposed TCL when the tunnel contents are intact involves compression of the tunnel contents too, and their response may be affected by, what Zheng *et al* (2006) describes as the boundary conditions. To an extent the three bony walls of the carpal tunnel present a solid boundary that limits the lateral and dorsal expansion of the tunnel contents during indentation; with only the proximal and distal tunnel openings allowing some expansion of tissue. This ‘confined compression’ may subsequently have an effect on measured variables.

In this current investigation, one specimen was tested in a 5th trial following removal of the tunnel contents ('TCL only'). Peak load (19.80 N) and stiffness (3.14 N/mm) values were much lower than 'TCL exposed'. A similar finding was also reported by Chaise *et al* (2003) when they tested their fresh frozen specimen with the tunnel contents removed (peak load: 7.4 to 10.1 N; stiffness: 14.5 to 21.7 N/mm). At first thought it might be said that these values are solely attributable to the TCL; however, this still may be somewhat inaccurate. The carpal arches of the specimens tested in the current study were not immobilised in any way; and it is possible that indentation of the TCL may also deform the carpal arch (Li *et al*, 2009; Xiu *et al*, 2010) rather than isolate the deformation to the TCL. An argument against this notion is that Holmes *et al* (2011) found no significant difference in carpal arch width at rest (29.3 ± 0.5 mm) and at peak load (28.7 ± 0.5 mm). However, the carpal arch width reported at peak load in their study is with the carpal tunnel contents still intact and this may prevent any large increase in concavity of the carpal arch when loaded in this manner.

6 Conclusion

The use of embalmed specimens for the determination of the mechanical properties of the soft tissue layers above the TCL is not recommended. Large variability in embalmed specimen quality can present erroneous results for peak loads and stiffness. However, the viscoelastic properties of embalmed specimens appear to be similar to those of fresh frozen tissue. The skin and adipose layer ('Intact' condition) showed slower load relaxations than any other tissue layer, while the muscular layer (the thenar muscle in particular) showed the fastest relaxation. The Thenar muscle group insertion on the TCL also provides more load absorption compared to that for the hypothenar muscle group. Peak loads and stiffness generally increased as each soft tissue layer was removed.

The test protocol used in this study presents limitations in attributing specific properties and characteristics to any one structure; and any characteristics determined (from the 'TCL exposed' level of testing) should be for the carpal tunnel complex as opposed to the TCL only.

6.1 De-limitations

The decision to use embalmed specimens in this study was mostly one of convenience. The author recognises that the mechanical properties of embalmed tissue are not wholly representative of *in-vivo*, or indeed, fresh frozen human tissue. Embalmed specimens were readily available for testing via the Laboratory of Human Anatomy, University of Glasgow; and present less of a biological hazard. It was the original intention of the investigation to include at least two fresh frozen specimens to allow some comparisons to be made with the results of the embalmed specimens. However, fresh frozen specimens were not available to the researchers for testing within the time constraints of this study.

The age of the donors always requires consideration in such investigations since research has found that the stiffness of human soft tissue generally increases with age

(Agache *et al.*, 1980); however, the age range of the specimen donors in this investigation is quite small (70 – 86 years of age, mean \pm SD: 82 \pm 6.29 yrs). The decision to test only one specimen for the ‘TCL only’ condition was due to the test protocol used in this investigation. To adequately test the TCL in isolation using the current indentation methodology would require immobilising the carpal arch and measuring changes in carpal arch width. Time constraints for this project prevented adequate pilot testing to develop a suitable protocol and would require that all conditions be tested with an immobilised carpal arch. The researcher preferred to test the specimens with the developed protocol used to better replicate *in-vivo* loading; as was used by Holmes *et al.* (2011).

The inclusion of the ‘Thenar removed’ and ‘Hypothenar removed’ tests was chosen to attempt to determine their contribution to the mechanics of the carpal tunnel complex. This resulted in the requirement to split the specimens into separate groups so that adequate comparison of mean scores between conditions could be performed; and subsequently reduced the sample size to three specimens per group. The author acknowledges that as a result of the smaller sample size, the power of any statistical analysis performed is compromised.

6.2 Limitations

Throughout the investigation various factors presented themselves that may have had an effect on the outcomes of the study.

A one hour recovery period between trials was implemented to control for hysteresis effects among the specimens. However, due to complications out with the control of the investigator; one specimen was tested over two consecutive days. Resulting in a period of 17 hours recovery between ‘Skin removed’ and ‘Hypothenar removed’ trials. This did not appear to have an adverse effect on the data recorded following the extended recovery period as the results for peak load and stiffness for that specimen were close to the mean of the group.

The method used to secure the hand specimens to the platform may have an effect on the data obtained. Increased pressure by the restraining bars on the flexor tendons proximal and distal to the carpal tunnel may cause a ‘bunching up’ effect of the

flexor tendons within the tunnel; furthermore, clamp pressures were not controlled for between trials.

It was the original intention of the author to compare the thickness of each layer of tissue to the results obtained at the respective levels of dissection. Unfortunately, an oversight by the author resulted in tissue layer thickness measurements not being fully recorded. Only 'Intact' palm thickness and 'TCL exposed' palm thickness were measured. As a result of this, and due to variability in specimen quality, it was decided not to perform correlation analysis between the outcome variables and anthropometric data. This is something that could be included in future investigations.

The test protocol developed for this investigation was inferred from those of similar studies (Chaise *et al*, 2003 and Holmes *et al*, 2011). However, as an aim of the investigation was to determine the mechanical and viscoelastic properties of the TCL and carpal tunnel, in order to further our understanding of the biomechanics of the wrist. The test protocol used does not adequately isolate the TCL and hence it is not possible to fully attribute any of the results obtained solely to the transverse carpal ligament.

6.3 Future Recommendation

Future research into the mechanical and viscoelastic properties of the TCL would need to better isolate the ligament, perhaps through dissection of the ligament and its four attaching carpal bones. The structure could then be mounted to fully immobilise the insertions of the TCL so that the ligament can be tested in isolation. A larger sample size of fresh cadaveric tissue is also recommended. Accurate, individual tissue layer properties should also be obtained through testing the tissues in isolation before comparing to those obtained here for validation.

Future studies into the biomechanics of the carpal arch should investigate the effects of the tunnel contents on the deformability of the carpal arch; with and without an intact TCL.

References

Agache PG, Monneur C, Leveque JL, and De Rigal J (1980) Mechanical Properties and Young's Modulus of Human Skin In Vivo. *Dermatological Research*. 269: 221-232.

Agur AMR and Dalley AF(2009) *Grant's Atlas of Anatomy: 11th edition*. Baltimore. Lippincott Williams and Wilkins.

Aroori S, and Spence RAJ (2008) Carpal Tunnel Syndrome. *Ulster Medical Journal*. 77(1): 6-17.

Berger JL (1993) Percutaneous Carpal Tunnel Plasty Method. U.S Pat. 5,179,963.

Bonifasi-Lista C, Lake SP , Small MS , and Weiss JA (2005) Viscoelastic Properties of the Human Medial Collateral Ligament Under Longitudinal, Transverse and Shear Loading. *Journal of Orthopaedic Research*. 23: 67-76.

Bower JA, Stanisz GJ, and Keir PJ (2006) An MRI Evaluation of Carpal Tunnel Dimensions in Healthy Wrists: Implications for Carpal Tunnel Syndrome. *Clinical Biomechanics*. 21: 816-825.

Chaise J, Ugbohue C, and Li ZM (2003) 'Viscoelastic Properties of the Transverse Carpal Ligament'. MRSC Summer Research Programme, University of Pittsburgh, U.S.A.

Chimich D, Shrive N, Frank C, Marchuk L, and Bray R (1992) Water Content Alters Viscoelastic Behaviour of the Normal Adolescent Rabbit Medial Collateral Ligament. *Journal of Biomechanics*. 25(8): 831-837.

Chrichton ML, Donose BC, Chen X, Raphael AP, Huang H, and Kendall MAF (2011) The Viscoelastic, Hyperelastic and Scale Dependant Behaviour of Freshly Excised Individual Skin Layers. *Biomaterials*. 32: 4670-4681.

Cobb TK, Dalley BK, Posteraro RH and Lewis RC (1993) Anatomy of the Flexor Retinaculum. *Journal of Hand Surgery-American Volume*. 18(1): 91-99. [Abstract].

Cobb TK, An K-N, Cooney WP, and Berger RA (1993a) Lumbrical Muscle Incursion into the Carpal Tunnel During Finger Flexion. *The journal of Hand Surgery: Journal of the British Society for Surgery of the Hand*. 19(4): 434-438.

Duenweld SE, Vanderby. Jr R, and Lakes RS (2009) Viscoelastic Relaxation and Recovery of Tendon. *Annals of Biomedical Engineering*. 37(6): 1131-1140.

Frank CB (2004) Ligament Structure, Physiology and Function. *Journal of Musculoskeletal Neuron Interaction*. 4(2): 199-201.

Geerligs M, Peters GWM, Ackermans PAJ, Oomens CWJ, and Baaijens FPT (2008) Linear Viscoelastic Behaviour of Subcutaneous Adipose Tissue. *Biorheology*. 45: 677-688.

Gellman H, Kan D, Gee V, Kuschner SH and Botte MJ (1989) Analysis of Pinch and Grip Strength After Carpal Tunnel Release. *The Journal of Hand Surgery*. 14(5): 863-864.

Holmes MWR, Howarth SJ, Callaghan JP, and Keir PJ (2011) Carpal Tunnel and Transverse Carpal Ligament Stiffness with Changes in Wrist Posture and Indenter Size. *Journal of Orthopaedic Research*. [Published online in Wiley Online Library (www.wileyonlinelibrary.com). DOI 10.1002/jor.21442] [Accessed: 15/06/2011].

Kiritsis PG and Kline SC (1995) Biomechanical Changes After Carpal Tunnel Release - A Cadaveric Model for Comparing Open, Endoscopic, and Step-Cut

Lengthening Techniques. *Journal Of Hand Surgery-American Volume*. 20A (2): 173-180. [Abstract].

Kline SC and Moore JR (1992) The Transverse Carpal Ligament. An Important Component of the Digital Flexor Pulley System. *The Journal of Bone and Joint Surgery*. 74: 1478-1485.

Li ZM (2005) Gender Difference in Carpal Tunnel Compliance. ISB XXth Congress - ASB 29th Annual Meeting (July 31 - August 5), Cleveland, Ohio. [Available online: <http://www.asbweb.org/conferences/2005/pdf/0265.pdf>] (Accessed: 20/03/2011).

Li ZM, Tang J, Chakan M, and Kaz R (2009) Carpal Tunnel Expansion by Palmarly Directed Forces to the Transverse Carpal Ligament. *Journal of Biomechanical Engineering*. 131(8): 081011 (6 Pages) [Abstract].

Li ZM, Masters TL, and Mondello TA (2011) Area and Shape Changes of the Carpal Tunnel in Response to Tunnel Pressure. *Journal of Orthopaedic Research*. [Published online in Wiley Online Library (wileyonlinelibrary.com). DOI 10.1002/jor.21468] Pages: 1-6. [Accessed: 15/05/2011).

Mathura K, Pynsenta PB, Vohraa SB, Thomasa B and Deshmukh SC (2004) Effect of wrist position on power grip and key pinch strength following carpal tunnel decompression. *Journal of Hand Surgery*. 29(4): 390-392.

Medical Dictionary. Definition: 'Ligament' and 'Retinaculum' [online] <<http://medical-dictionary.thefreedictionary.com/ligament>> (or retinaculum). (Accessed 19/07/2011).

Middleton WD, Kneeland JB, Kellman GM, Cates JD, Sanger JR, Jesmanowicz A, Froncisz W and Hyde JS (1987) MR Imaging of the Carpal Tunnel: Normal

Anatomy and Preliminary Findings in the Carpal Tunnel Syndrome. *American Journal of Roentgenology*. 148(2): 307-316.

Miller-Young JE, Duncan NA, and Baroud G (2002) Material Properties of the Human Calcaneal Fat Pad in Compression: Experiment and Theory. *Journal of Biomechanics*. 35: 1523-1531.

NHS Choices. Carpal Tunnel Syndrome.

<http://www.nhs.uk/conditions/carpal-tunnel-syndrome/Pages/Whatisitfinal.aspx>
(accessed 10 Mar 2011).

Pacek CA, Chakan M, Goitz RJ, Kaufmann RA and Li ZM (2010) Morphological Analysis of the Transverse Carpal Ligament. *American Association of Hand Surgery*. 5 (2): 135-140.

Provenzano P, Lakes R, Keenan T, and Vanderby Jr R (2001) Nonlinear Ligament Viscoelasticity. *Annals of Biomedical Engineering*. 29:908-914.

SilverThorn MB (1999) *In-Vivo* Indentation of Lower Extremity Limb Soft Tissues. *IEEE Transactions of Rehabilitation Engineering*. 7(3): 268-277.

Smalls LK, Wickett RR, and Visscher MO (2006) The Effect of Dermal Thickness, Tissue Composition, and Body Site on Skin Biomechanical Properties. *Skin Research and Technology*. 12: 43-49.

Stecco C, Macchi V, Lancerotto L, Tiengo C, Porzionato A and De Caro R (2010) Comparison of Transverse Carpal Ligament and Flexor Retinaculum Terminology for the Wrist. *The Journal of Hand Surgery*. 35 (5): 746-753.

Sucher BM, Hinrichs RN, Welcher RL, and Quiroz L-D (2005) Manipulative Treatment of Carpal Tunnel Syndrome: Biomechanical and Osteopathic Intervention to Increase the Length of the Transverse Carpal Ligament: Part 2. Effect of Sex

Differences and Manipulative “Priming”. *Journal of the American Osteopathic Association*. 105(3): 135-143.

Tanabe T, and Okutsu I (1997) An Anatomical Study of the Palmar Ligamentous Structures of the Carpal Canal. *The Journal of Hand Surgery: Journal of the British Society for Surgery of the Hand*. 22(6): 754-757. [Abstract].

Tengrootenhuysen M, Van Riet R, Pimontel P, Bortier H and Glabbeek F (2009) The Role of the Transverse Carpal Ligament in Carpal Stability: an in-vitro study. *Acta Orthopaedica Belgica*. 75(4): 467-471. [Abstract].

Uchiyama S, Yasutomi T, Momose T, Nakagawa H, Kamimura M, and Kato H (2010) Carpal Tunnel Pressure Measurement During Two-Portal Endoscopic Carpal Tunnel Release. *Clinical Biomechanics*. 25: 893-898.

Van Loocke M, Lyons CG, and Simms CK (2008) Viscoelastic Properties of Passive Skeletal Muscle in Compression: Stress-Relaxation Behaviour and Constitutive Modelling. *Journal of Biomechanics*. 41: 1555-1566.

Viidik A and Lewin T (1966) Changes in Tensile Strength Characteristics and Histology of Rabbit Ligaments Induced by Different Modes of Postmortal Storage. *Acta Orthopaedica Scandinavia*. 37: 141-155.

Weiss JA, Gardiner JC, and Bonifasi-Lista C (2002) Ligament Material Behaviour is non-linear, Viscoelastic and Rate-dependent Under Shear Loading. *Journal of Biomechanics*. 35: 943-950.

Wilke HJ, Kirschack s, and Claes LE (1996) Formalin Fixation Strongly Influences Biomechanical Properties of the Spine. *Journal of Biomechanics*. 29(12): 1629-1631.

Xiu KH, Kim JH and Li ZM (2010) Biomechanics of the Transverse Carpal Arch Under Carpal Bone Loading. *The Journal of Clinical Biomechanics*. 25: 776-780.

Yu HL, Chase RA and Strauch B (2004) *Atlas of Hand Anatomy and Clinical Implications*. St. Louis, Missouri. Mosby.

Zheng YP, Li ZM, Choi APC, Lu MH, Chen X, and Huang QH (2006) Ultrasound Palpation Sensor for Tissue Thickness and Elasticity Measurements – Assessment of Transverse Carpal Ligament. *Ultrasonics*. 44: 313-317.

Appendix A: Material Photos

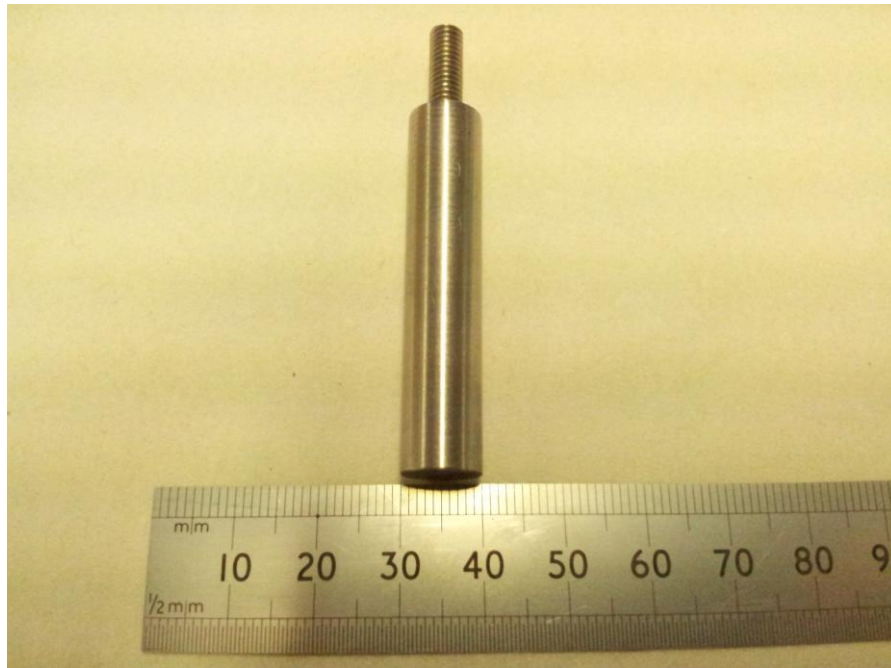


Figure 9: Custom made 10 mm diameter aluminium indenter

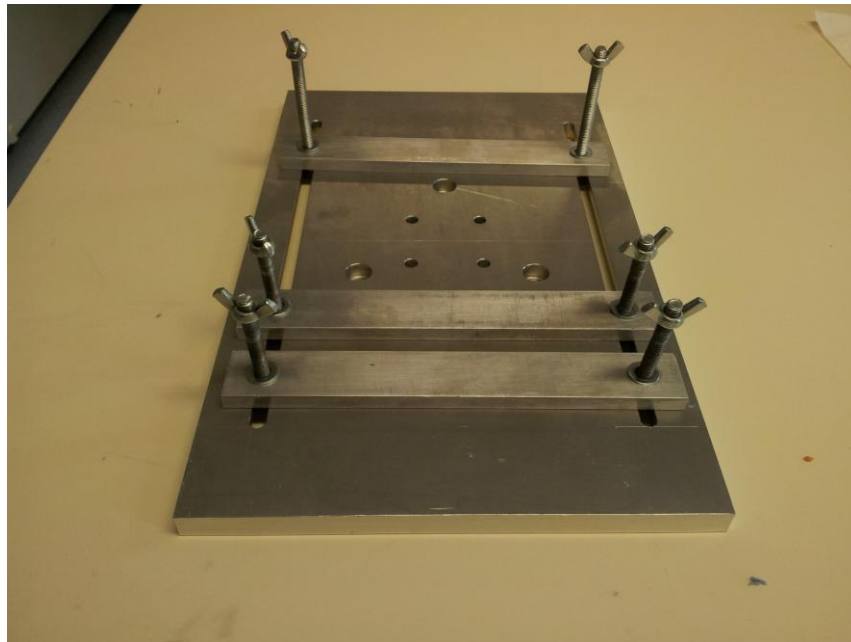


Figure 10: Custom made aluminium specimen platform. Dimensions: overall width: 250 mm; length: 400mm; depth: 15mm; bolt grooves: 25mm indent from side, 300mm length, 8mm width. Restraining bars (x3): width: 32mm; length: 233mm; depth: 10mm. Bolts: 8mm threaded bolts with wing nuts.

Appendix B: Indenter Location Guide

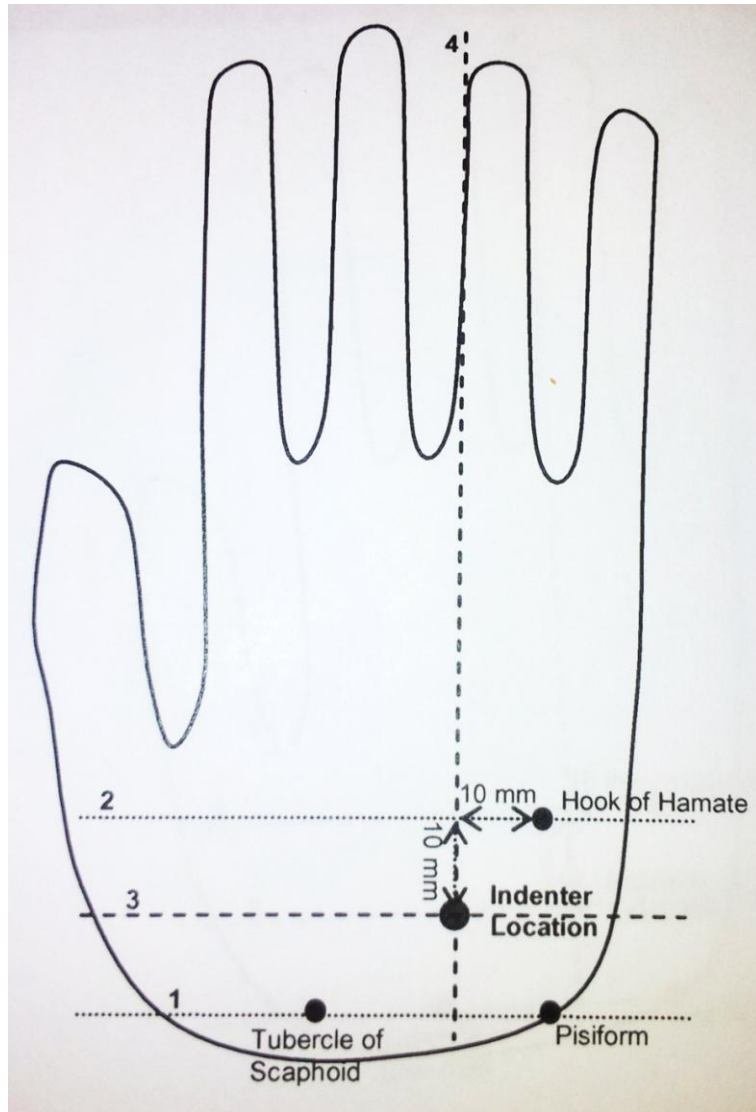


Figure 11: Location of TCL centre of intact hand

Appendix C: Dissection level Images



Figure 12: Intact Hand with TCL centre located



Figure 13: Skin, subcutaneous adipose and palmar aponeurosis removed



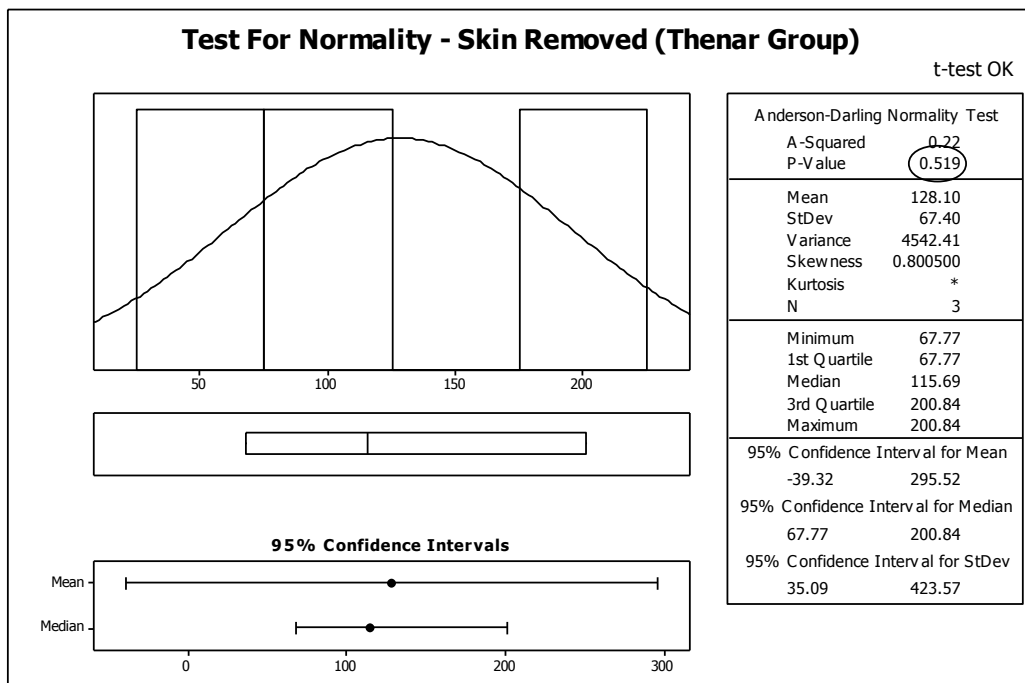
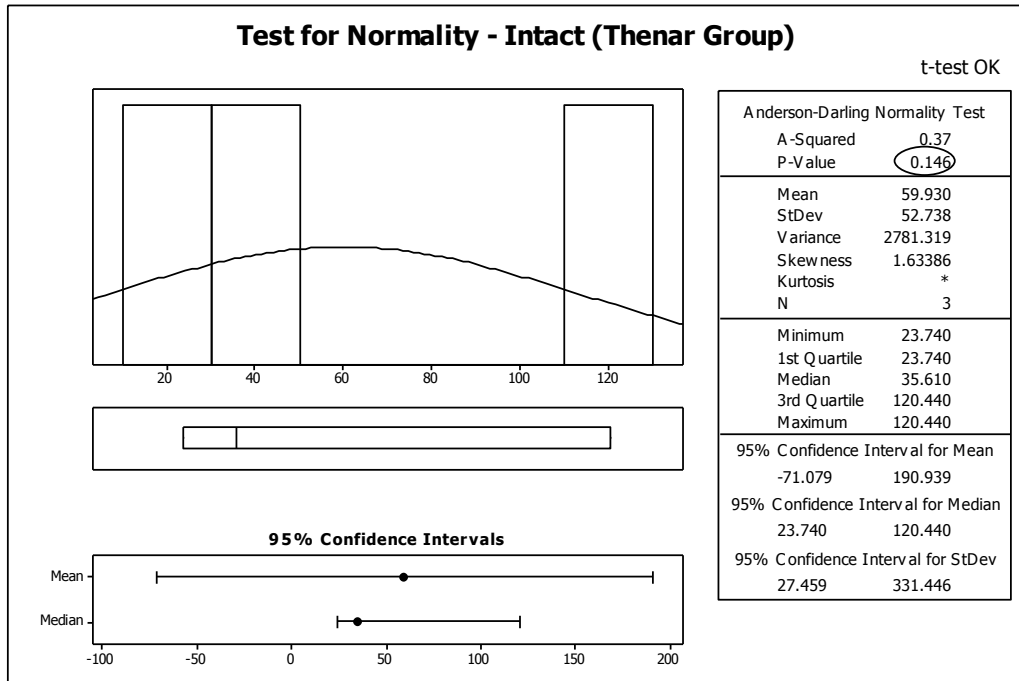
Figure 14: Thenar Muscle Group Removed



Figure 15: TCL Exposed

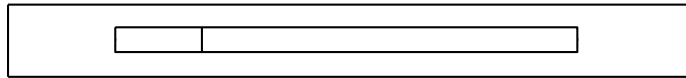
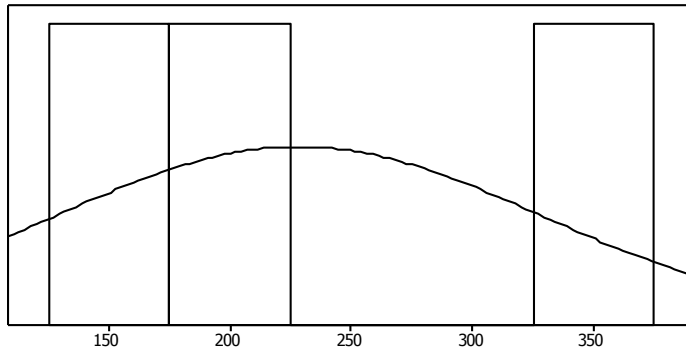
Appendix D: Anderson-Darling Normality Tests

Normality graphs for Peak Load

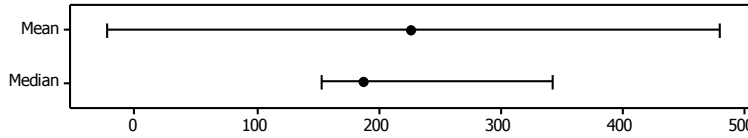


Test for Normality - Thenar Removed

t-test OK



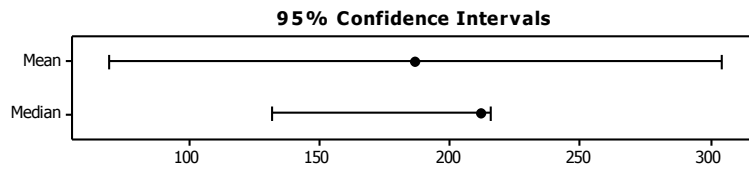
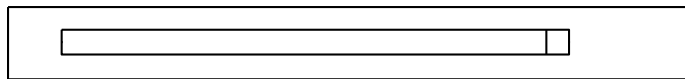
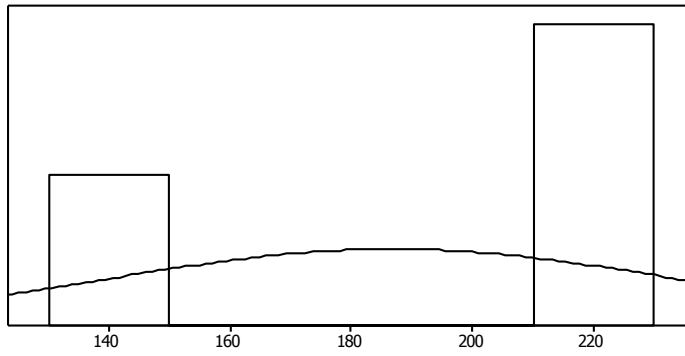
95% Confidence Intervals



Anderson-Darling Normality Test	
A-Squared	0.32
P-Value	0.229
Mean	228.15
StDev	101.18
Variance	10236.55
Skewness	1.49578
Kurtosis	*
N	3
Minimum	152.91
1st Quartile	152.91
Median	188.37
3rd Quartile	343.17
Maximum	343.17
95% Confidence Interval for Mean	-23.18 479.48
95% Confidence Interval for Median	152.91 343.17
95% Confidence Interval for StDev	52.68 635.86

Test for Normality - TCL Exposed (Thenar Group)

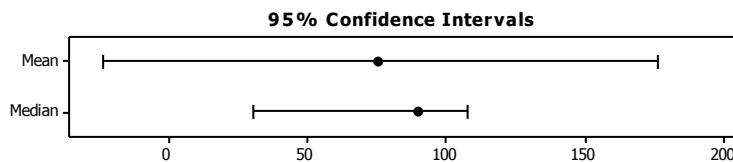
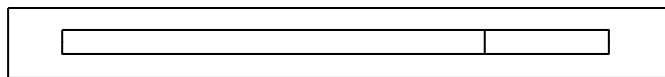
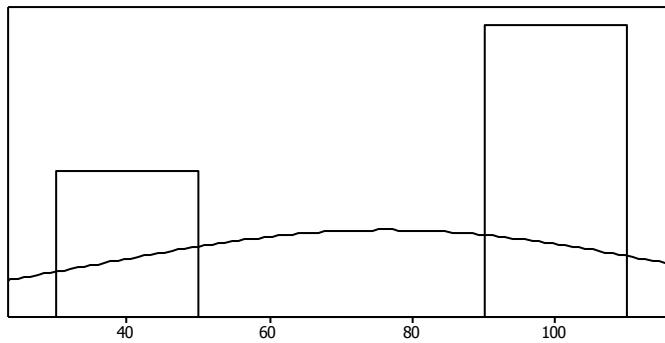
t-test OK



Anderson-Darling Normality Test	
A-Squared	0.45
P-Value	0.080
Mean	186.77
StDev	47.32
Variance	2238.78
Skewness	-1.72096
Kurtosis	*
N	3
Minimum	132.17
1st Quartile	132.17
Median	212.28
3rd Quartile	215.85
Maximum	215.85
95% Confidence Interval for Mean	
	69.23 304.31
95% Confidence Interval for Median	
	132.17 215.85
95% Confidence Interval for StDev	
	24.64 297.37

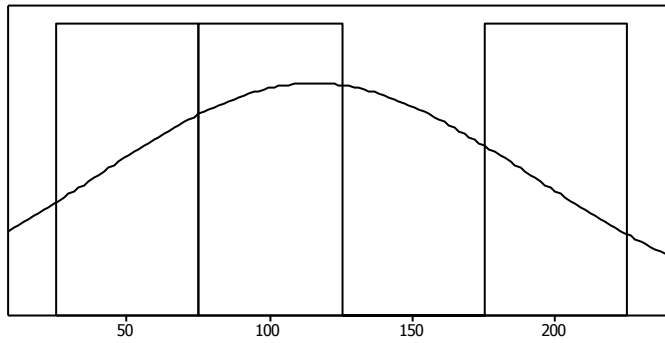
Test for Normality - Intact (Hypothenar Group)

t-test OK



Anderson-Darling Normality Test	
A-Squared	0.29
P-Value	0.294
Mean	76.110
StDev	40.213
Variance	1617.058
Skewness	-1.37321
Kurtosis	*
N	3
Minimum	30.780
1st Quartile	30.780
Median	90.060
3rd Quartile	107.490
Maximum	107.490
95% Confidence Interval for Mean	
	-23.784 176.004
95% Confidence Interval for Median	
	30.780 107.490
95% Confidence Interval for StDev	
	20.937 252.726

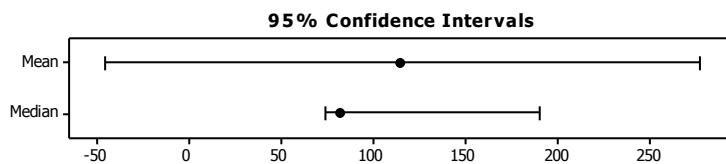
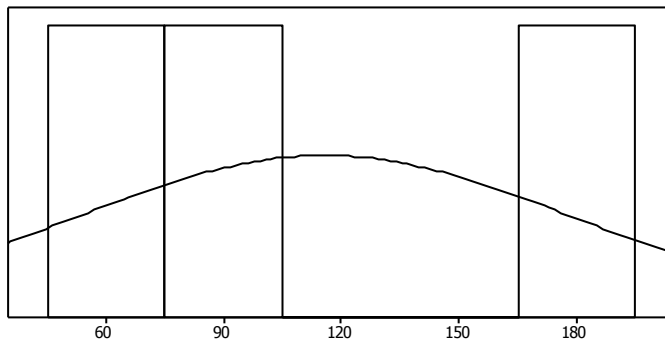
Test for Normality - Skin Removed (Hypothenar Group)



t-test OK

Anderson-Darling Normality Test	
A-Squared	0.32
P-Value	0.239
Mean	115.48
StDev	75.39
Variance	5683.19
Skewness	1.47766
Kurtosis	*
N	3
Minimum	58.97
1st Quartile	58.97
Median	86.40
3rd Quartile	201.08
Maximum	201.08
95% Confidence Interval for Mean	-71.79 302.75
95% Confidence Interval for Median	58.97 201.08
95% Confidence Interval for StDev	39.25 473.79

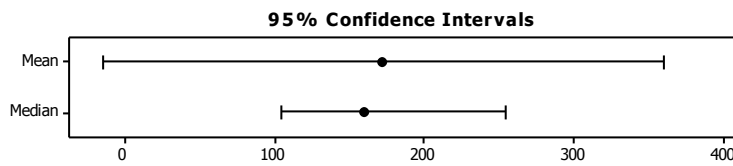
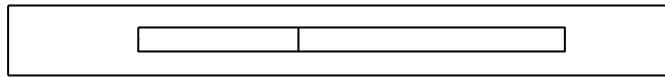
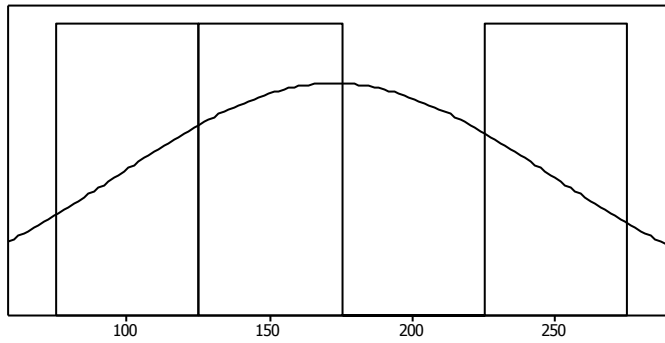
Test for Normality - Hypothenar Removed



t-test OK

Anderson-Darling Normality Test	
A-Squared	0.43
P-Value	0.096
Mean	115.71
StDev	64.90
Variance	4212.60
Skewness	1.70467
Kurtosis	*
N	3
Minimum	74.45
1st Quartile	74.45
Median	82.15
3rd Quartile	190.52
Maximum	190.52
95% Confidence Interval for Mean	-45.53 276.94
95% Confidence Interval for Median	74.45 190.52
95% Confidence Interval for StDev	33.79 407.91

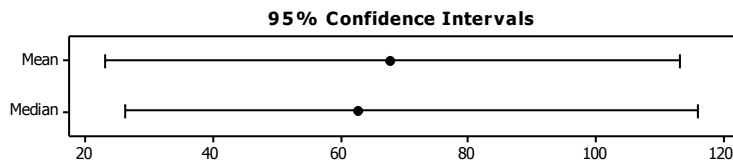
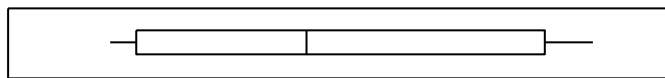
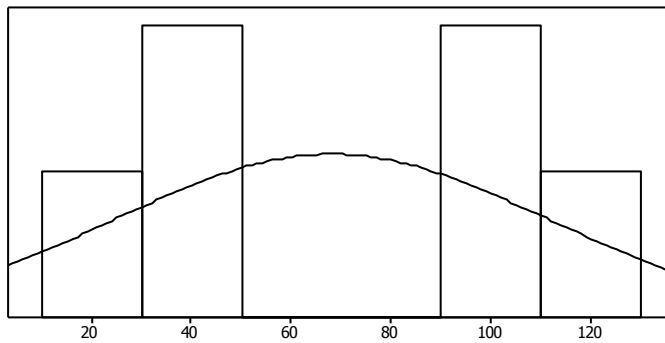
Test for Normality - TCL Exposed (Hypothenar Group)



t-test OK

Anderson-Darling Normality Test	
A-Squared	0.21
P-Value	0.535
Mean	172.51
StDev	75.39
Variance	5684.40
Skewness	0.725016
Kurtosis	*
N	3
Minimum	104.14
1st Quartile	104.14
Median	160.02
3rd Quartile	253.37
Maximum	253.37
95% Confidence Interval for Mean	-14.78 359.80
95% Confidence Interval for Median	104.14 253.37
95% Confidence Interval for StDev	39.26 473.84

Test for Normality - Intact_All

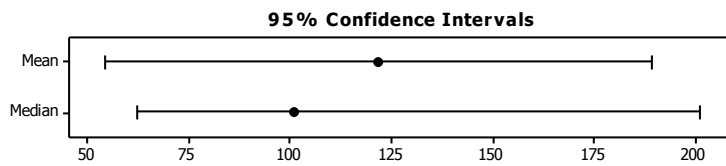
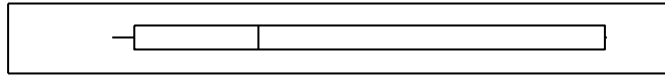
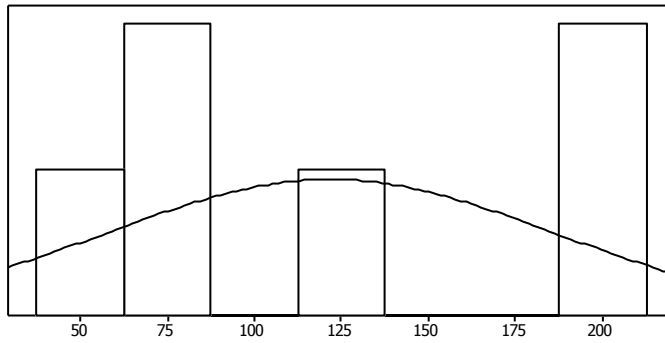


t-test OK

Anderson-Darling Normality Test	
A-Squared	0.45
P-Value	0.167
Mean	68.020
StDev	42.871
Variance	1837.889
Skewness	0.16650
Kurtosis	-2.70948
N	6
Minimum	23.740
1st Quartile	29.020
Median	62.835
3rd Quartile	110.728
Maximum	120.440
95% Confidence Interval for Mean	23.030 113.010
95% Confidence Interval for Median	26.254 115.815
95% Confidence Interval for StDev	26.760 105.145

Test for Normality - Skin Removed (All Specimens)

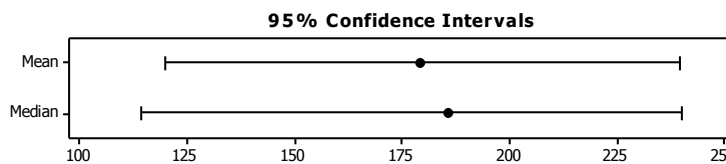
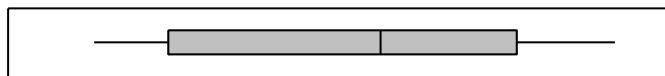
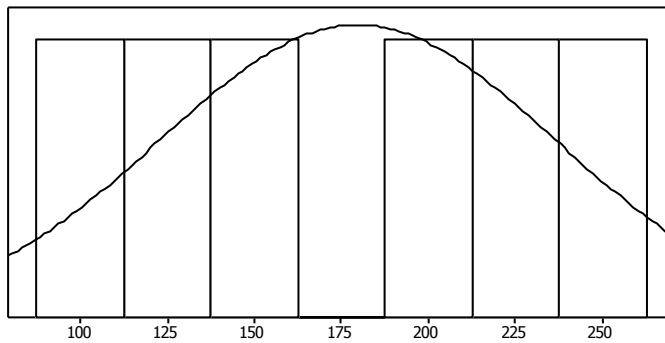
t-test OK



Anderson-Darling Normality Test	
A-Squared	0.48
P-Value	0.142
Mean	121.79
StDev	64.33
Variance	4138.00
Skewness	0.61115
Kurtosis	-1.98902
N	6
Minimum	58.97
1st Quartile	65.57
Median	101.05
3rd Quartile	200.90
Maximum	201.08
95% Confidence Interval for Mean	
	54.28 189.30
95% Confidence Interval for Median	
	62.11 200.99
95% Confidence Interval for StDev	
	40.15 157.77

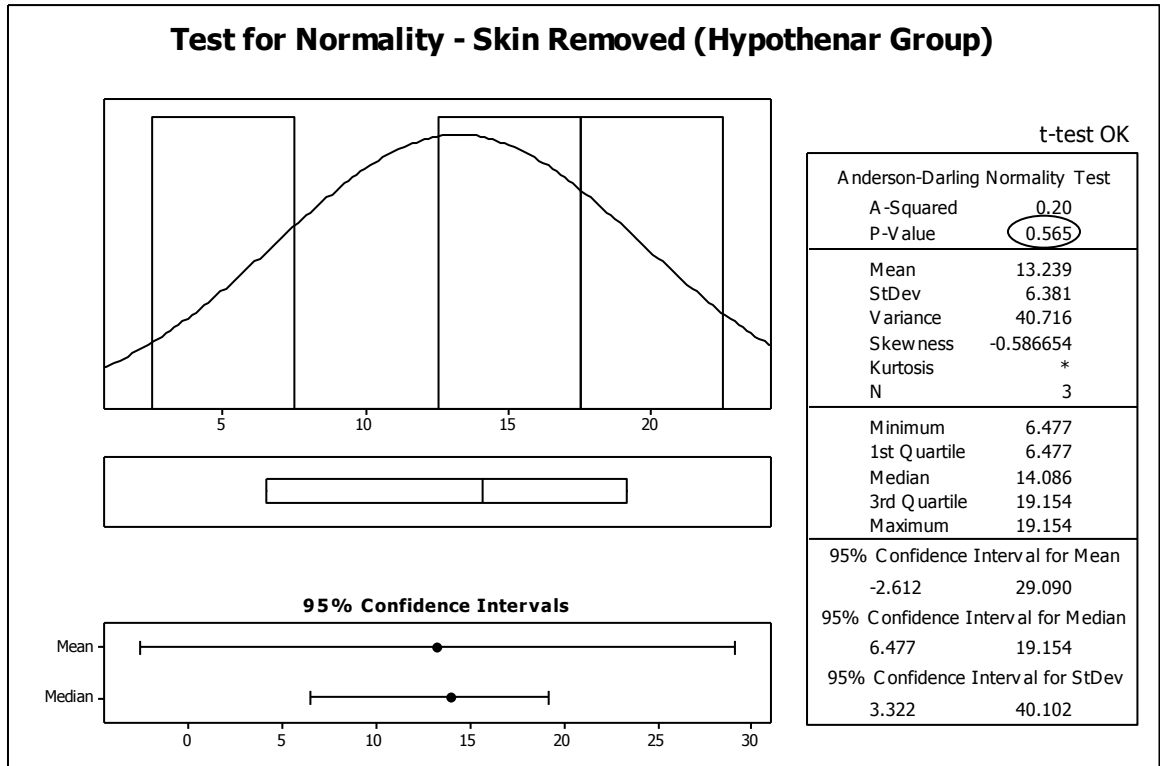
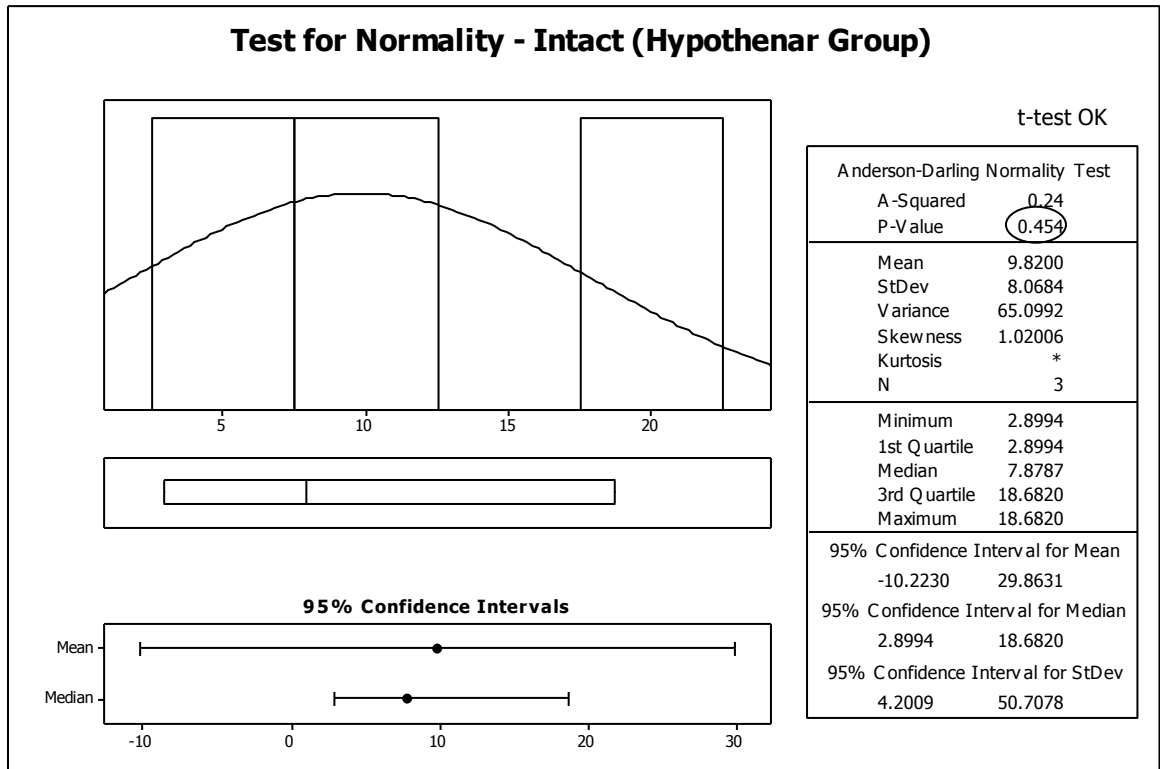
Test for Normality-TCL Exposed (All Specimens)

t-test OK

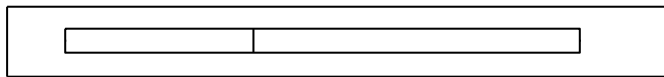
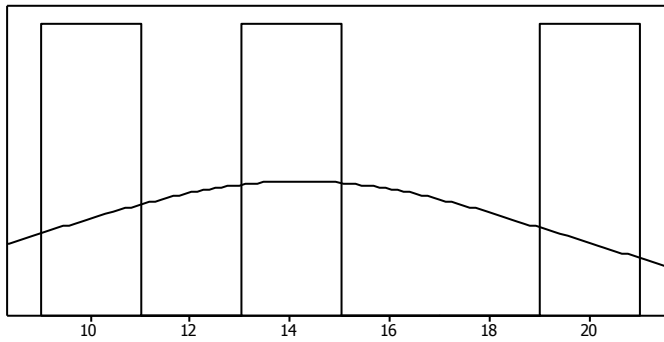


Anderson-Darling Normality Test	
A-Squared	0.22
P-Value	0.690
Mean	179.64
StDev	56.84
Variance	3230.25
Skewness	-0.10091
Kurtosis	-1.54573
N	6
Minimum	104.14
1st Quartile	125.16
Median	186.15
3rd Quartile	225.23
Maximum	253.37
95% Confidence Interval for Mean	
	119.99 239.28
95% Confidence Interval for Median	
	114.15 239.97
95% Confidence Interval for StDev	
	35.48 139.39

Normality Graphs for Stiffness



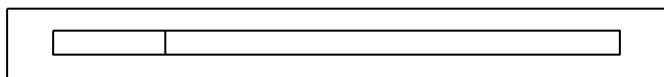
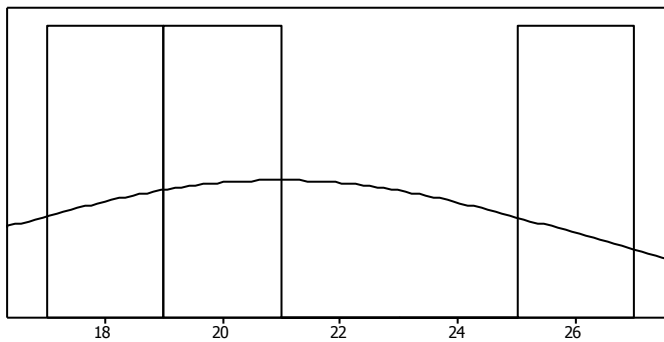
Test for Normality - Hypothenar Removed



t-test OK

Anderson-Darling Normality Test	
A-Squared	0.22
P-Value	0.526
Mean	14.193
StDev	5.210
Variance	27.142
Skewness	0.768826
Kurtosis	*
N	3
Minimum	9.503
1st Quartile	9.503
Median	13.274
3rd Quartile	19.801
Maximum	19.801
95% Confidence Interval for Mean	1.251 27.134
95% Confidence Interval for Median	9.503 19.801
95% Confidence Interval for StDev	2.713 32.742

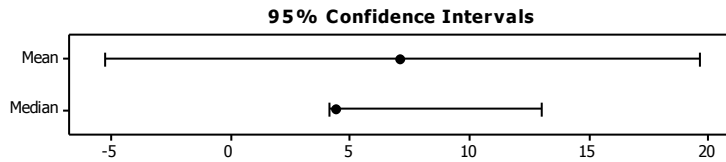
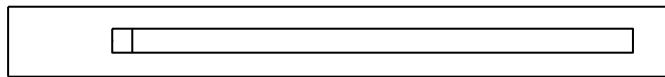
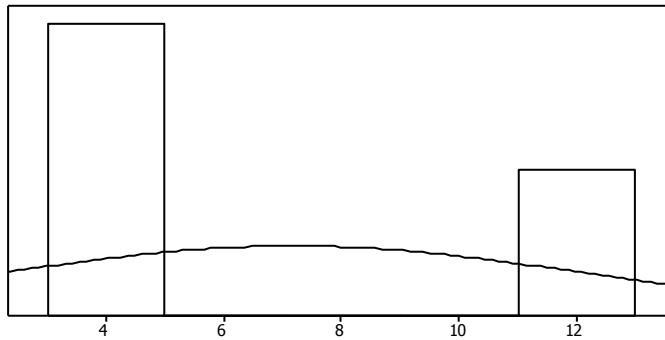
Test for Normality - TCL Exposed (Hypothenar Group)



t-test OK

Anderson-Darling Normality Test	
A-Squared	0.31
P-Value	0.248
Mean	20.961
StDev	5.093
Variance	25.935
Skewness	1.45944
Kurtosis	*
N	3
Minimum	17.114
1st Quartile	17.114
Median	19.033
3rd Quartile	26.736
Maximum	26.736
95% Confidence Interval for Mean	8.310 33.612
95% Confidence Interval for Median	17.114 26.736
95% Confidence Interval for StDev	2.652 32.006

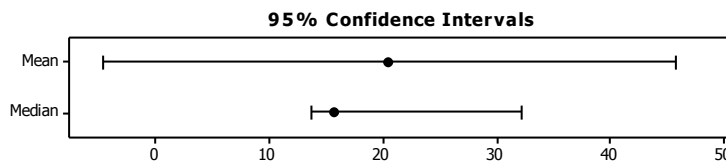
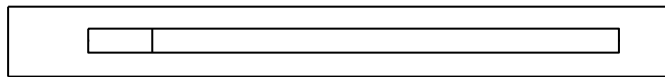
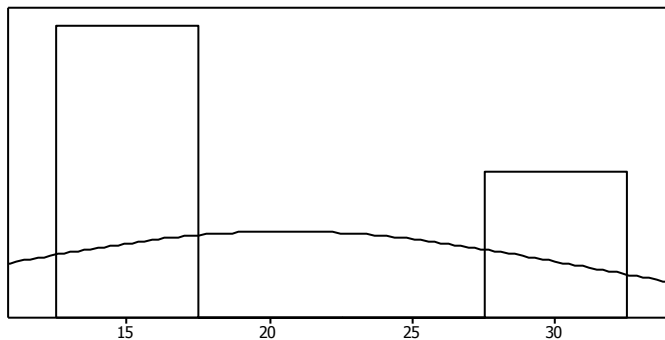
Test for Normality - Intact (Thenar Group)



t-test OK

Anderson-Darling Normality Test	
A-Squared	0.45
P-Value	0.079
Mean	7.1729
StDev	5.0221
Variance	25.2216
Skewness	1.72161
Kurtosis	*
N	3
Minimum	4.0914
1st Quartile	4.0914
Median	4.4592
3rd Quartile	12.9680
Maximum	12.9680
95% Confidence Interval for Mean	-5.3027 19.6485
95% Confidence Interval for Median	4.0914 12.9680
95% Confidence Interval for StDev	2.6148 31.5626

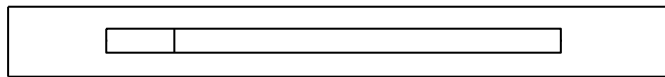
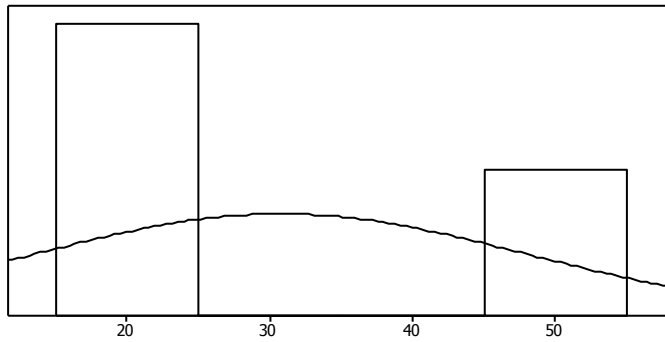
Test for Normality - Skin Removed (Thenar Group)



t-test OK

Anderson-Darling Normality Test	
A-Squared	0.38
P-Value	0.142
Mean	20.566
StDev	10.129
Variance	102.601
Skewness	1.63929
Kurtosis	*
N	3
Minimum	13.645
1st Quartile	13.645
Median	15.861
3rd Quartile	32.192
Maximum	32.192
95% Confidence Interval for Mean	-4.597 45.728
95% Confidence Interval for Median	13.645 32.192
95% Confidence Interval for StDev	5.274 63.660

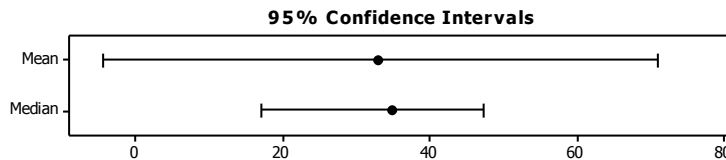
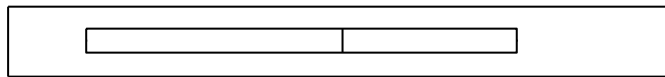
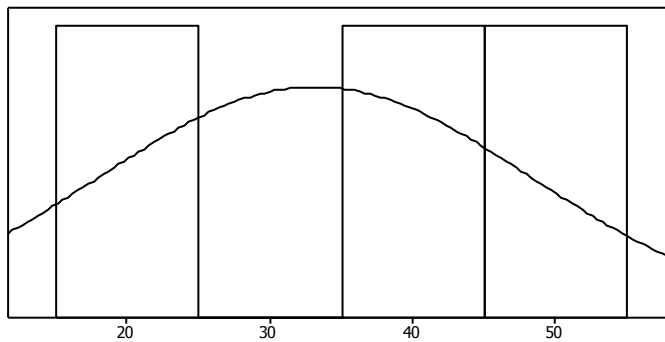
Test for Normality - Thenar Removed



t-test OK

Anderson-Darling Normality Test	
A-Squared	0.35
P-Value	0.181
Mean	30.733
StDev	17.174
Variance	294.931
Skewness	1.57819
Kurtosis	*
N	3
Minimum	18.494
1st Quartile	18.494
Median	23.340
3rd Quartile	50.365
Maximum	50.365
95% Confidence Interval for Mean	-11.928 73.395
95% Confidence Interval for Median	18.494 50.365
95% Confidence Interval for StDev	8.942 107.931

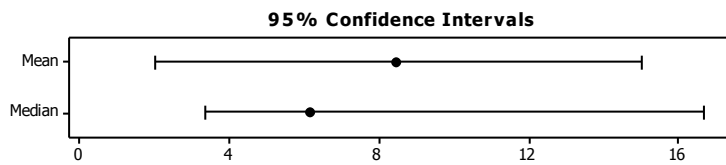
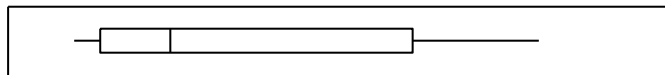
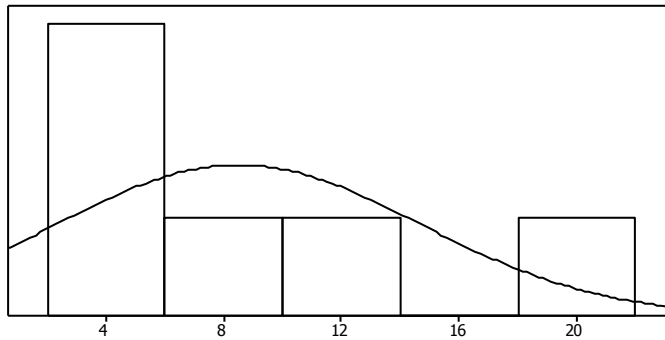
Test for Normality - TCL Exposed (Thenar Group)



t-test OK

Anderson-Darling Normality Test	
A-Squared	0.20
P-Value	0.570
Mean	33.138
StDev	15.153
Variance	229.615
Skewness	-0.563781
Kurtosis	*
N	3
Minimum	17.112
1st Quartile	17.112
Median	35.068
3rd Quartile	47.234
Maximum	47.234
95% Confidence Interval for Mean	-4.504 70.780
95% Confidence Interval for Median	17.112 47.234
95% Confidence Interval for StDev	7.890 95.233

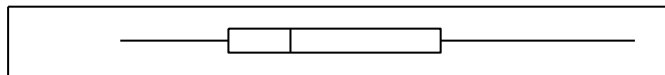
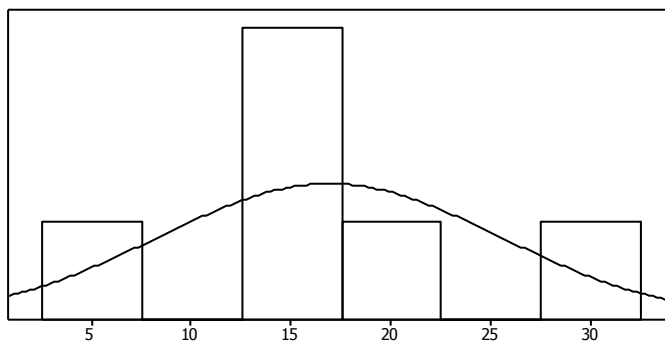
Test for Normality Intact (All Specimens)



t-test OK

Anderson-Darling Normality Test	
A-Squared	0.40
P-Value	0.246
Mean	8.4964
StDev	6.1831
Variance	38.2306
Skewness	1.03974
Kurtosis	-0.12602
N	6
Minimum	2.8994
1st Quartile	3.7934
Median	6.1689
3rd Quartile	14.3965
Maximum	18.6820
95% Confidence Interval for Mean	2.0077 14.9852
95% Confidence Interval for Median	3.3251 16.6413
95% Confidence Interval for StDev	3.8595 15.1647

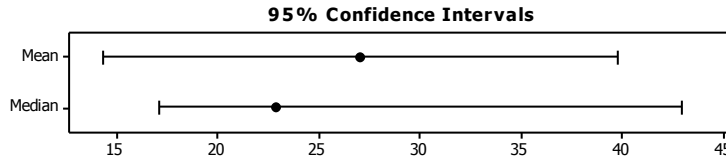
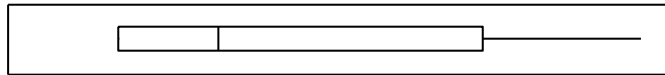
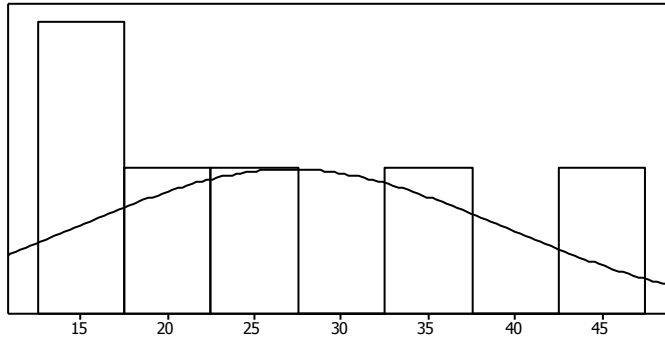
Test for Normality - Skin Removed (All Specimens)



t-test OK

Anderson-Darling Normality Test	
A-Squared	0.39
P-Value	0.259
Mean	16.903
StDev	8.569
Variance	73.430
Skewness	1.14157
Kurtosis	2.40400
N	6
Minimum	6.477
1st Quartile	11.853
Median	14.973
3rd Quartile	22.414
Maximum	32.192
95% Confidence Interval for Mean	7.910 25.895
95% Confidence Interval for Median	9.037 27.536
95% Confidence Interval for StDev	5.349 21.017

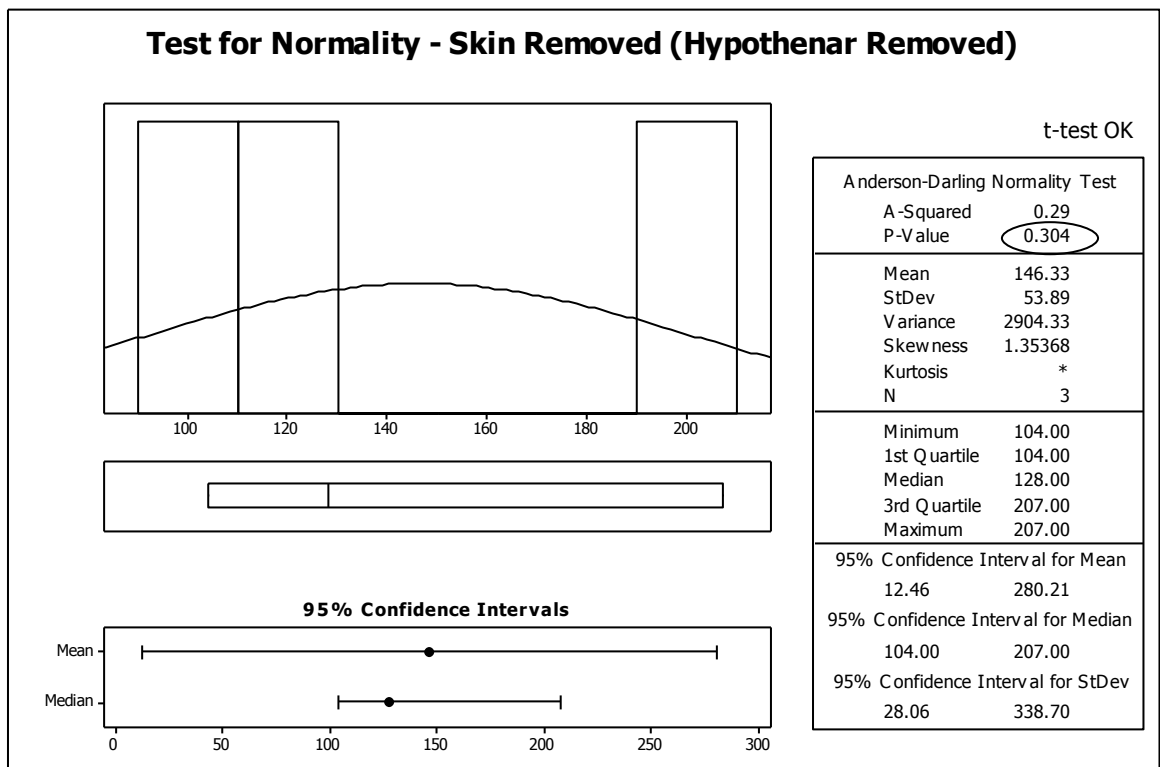
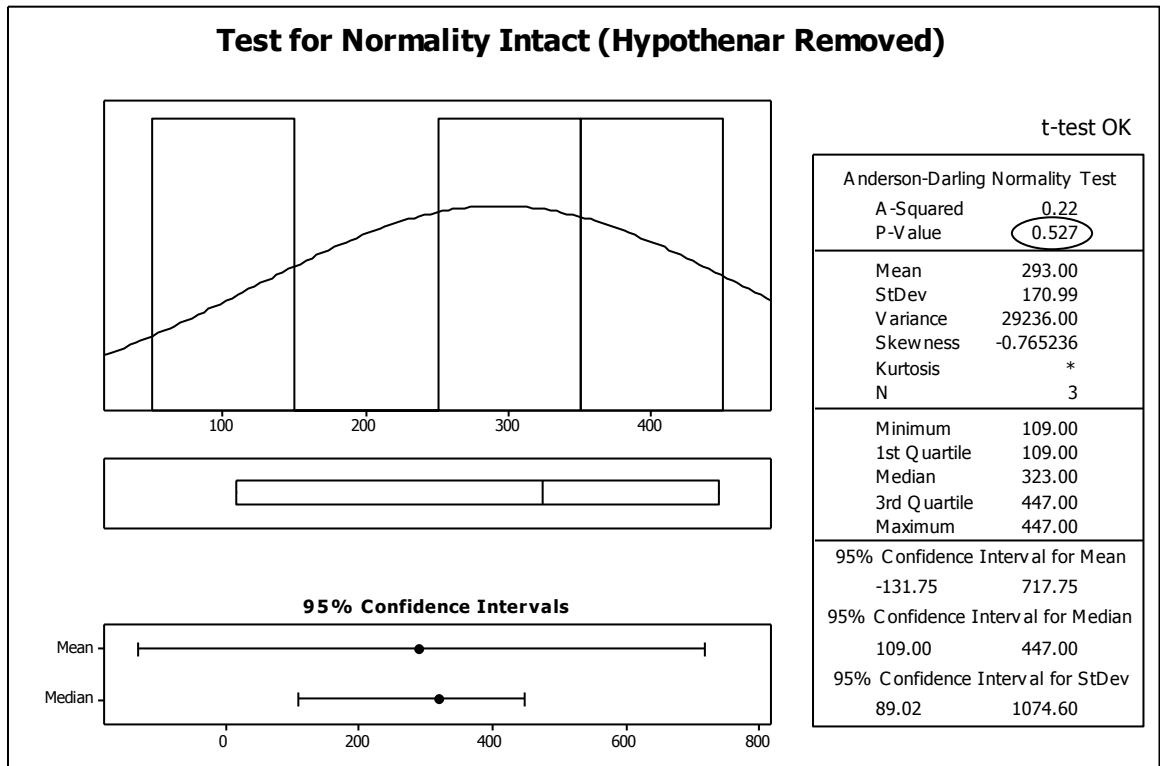
Test for Normality - TCL Exposed (All Specimens)



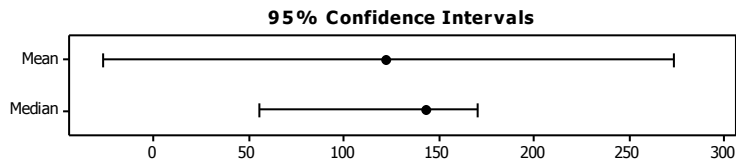
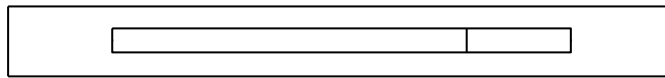
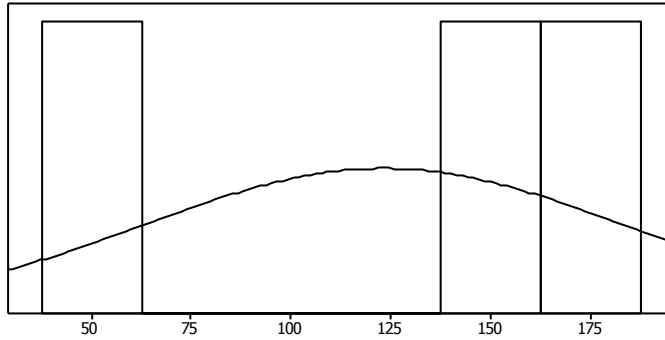
t-test OK

Anderson-Darling Normality Test	
A-Squared	0.42
P-Value	0.209
Mean	27.049
StDev	12.112
Variance	146.701
Skewness	1.05713
Kurtosis	0.05126
N	6
Minimum	17.112
1st Quartile	17.114
Median	22.885
3rd Quartile	38.109
Maximum	47.234
95% Confidence Interval for Mean	
	14.339 39.760
95% Confidence Interval for Median	
	17.113 42.889
95% Confidence Interval for StDev	
	7.560 29.706

Normality Graphs: Relaxation Time



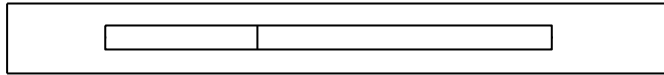
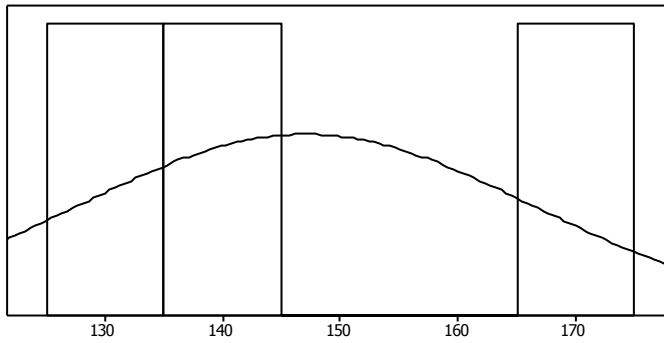
Test for Normality - Hypothetar Removed



t-test OK

Anderson-Darling Normality Test	
A-Squared	0.29
P-Value	0.292
Mean	123.00
StDev	60.31
Variance	3637.00
Skewness	-1.37697
Kurtosis	*
N	3
Minimum	55.00
1st Quartile	55.00
Median	144.00
3rd Quartile	170.00
Maximum	170.00
95% Confidence Interval for Mean	
	-26.81 272.81
95% Confidence Interval for Median	
	55.00 170.00
95% Confidence Interval for StDev	
	31.40 379.02

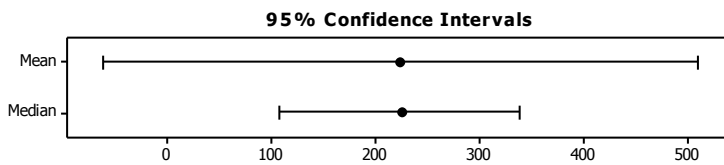
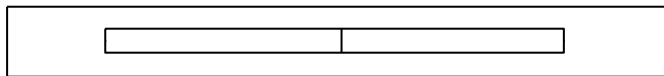
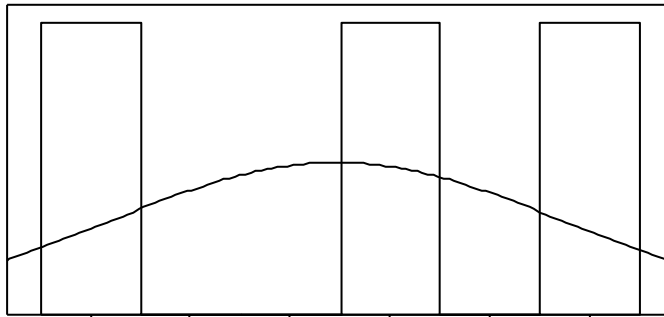
Test for Normality - TCL Exposed (Hypothenar Group)



t-test OK

Anderson-Darling Normality Test	
A-Squared	0.23
P-Value	0.503
Mean	147.00
StDev	19.31
Variance	373.00
Skewness	0.892026
Kurtosis	*
N	3
Minimum	130.00
1st Quartile	130.00
Median	143.00
3rd Quartile	168.00
Maximum	168.00
95% Confidence Interval for Mean	99.02 194.98
95% Confidence Interval for Median	130.00 168.00
95% Confidence Interval for StDev	10.06 121.38

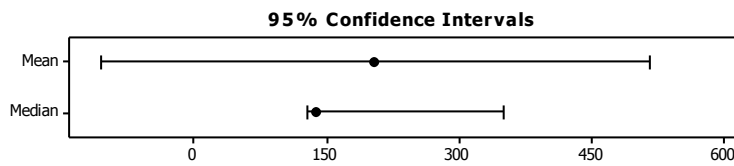
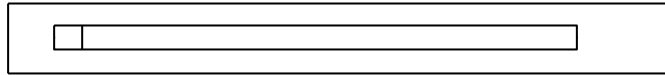
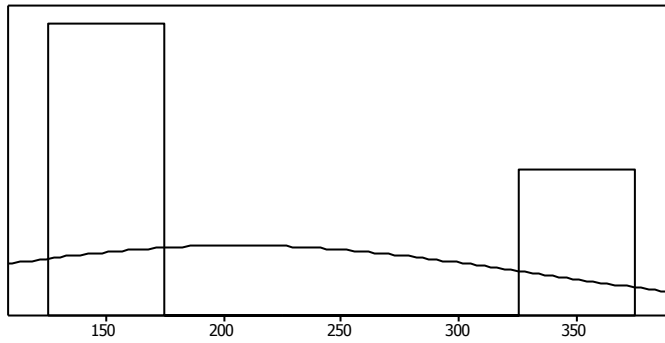
Test for Normality - Skin Removed (Thenar Group)



t-test OK

Anderson-Darling Normality Test	
A-Squared	0.19
P-Value	0.630
Mean	223.00
StDev	115.01
Variance	13228.00
Skewness	-0.0782283
Kurtosis	*
N	3
Minimum	107.00
1st Quartile	107.00
Median	225.00
3rd Quartile	337.00
Maximum	337.00
95% Confidence Interval for Mean	-62.71 508.71
95% Confidence Interval for Median	107.00 337.00
95% Confidence Interval for StDev	59.88 722.83

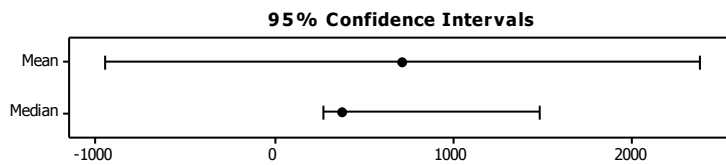
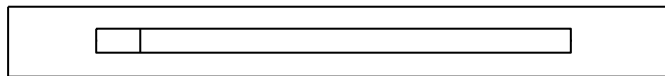
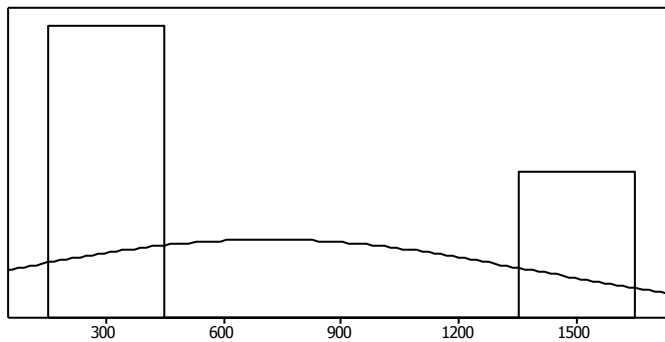
Test for Normality - Thenar Removed



t-test OK

Anderson-Darling Normality Test	
A-Squared	0.44
P-Value	0.087
Mean	206.00
StDev	124.85
Variance	15588.00
Skewness	1.71407
Kurtosis	*
N	3
Minimum	128.00
1st Quartile	128.00
Median	140.00
3rd Quartile	350.00
Maximum	350.00
95% Confidence Interval for Mean	-104.15 516.15
95% Confidence Interval for Median	128.00 350.00
95% Confidence Interval for StDev	65.01 784.66

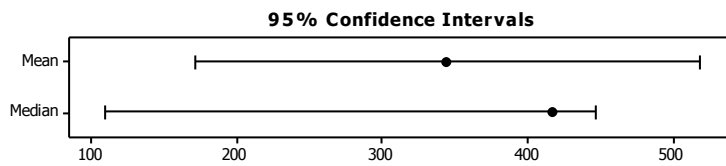
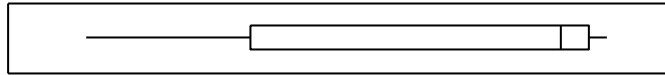
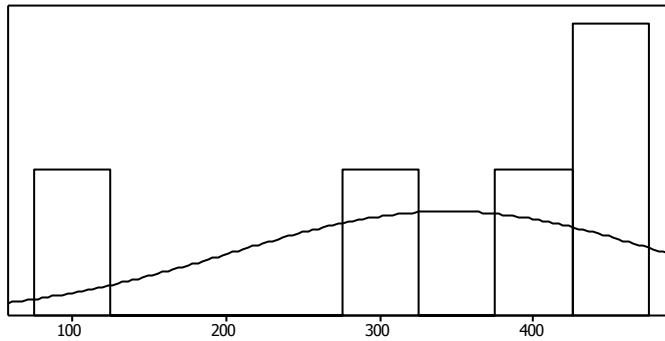
Test for Normality - TCL Exposed (Thenar Group)



t-test OK

Anderson-Darling Normality Test	
A-Squared	0.40
P-Value	0.118
Mean	714.67
StDev	670.34
Variance	449352.33
Skewness	1.67781
Kurtosis	*
N	3
Minimum	273.00
1st Quartile	273.00
Median	385.00
3rd Quartile	1486.00
Maximum	1486.00
95% Confidence Interval for Mean	-950.54 2379.88
95% Confidence Interval for Median	273.00 1486.00
95% Confidence Interval for StDev	349.02 4212.89

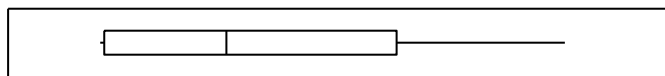
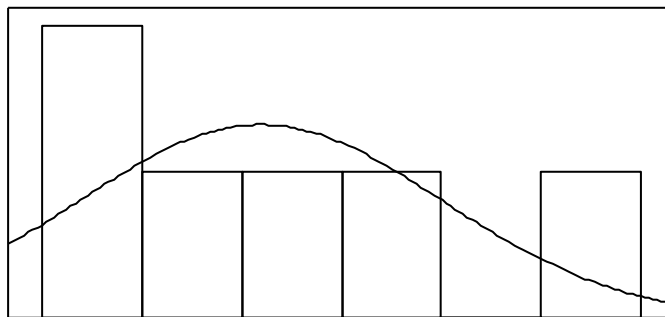
Test for Normality - Intact (All Specimens)



t-test OK

Anderson-Darling Normality Test	
A-Squared	0.56
P-Value	0.072
Mean	344.40
StDev	139.92
Variance	19577.80
Skewness	-1.68102
Kurtosis	2.60941
N	5
Minimum	109.00
1st Quartile	216.00
Median	418.00
3rd Quartile	436.00
Maximum	447.00
95% Confidence Interval for Mean	
	170.67 518.13
95% Confidence Interval for Median	
	109.00 447.00
95% Confidence Interval for StDev	
	83.83 402.07

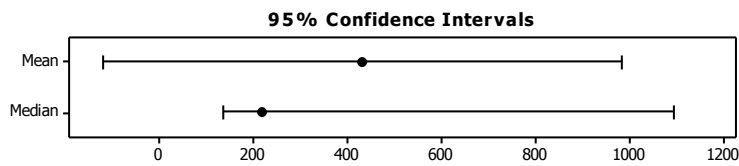
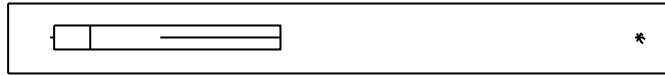
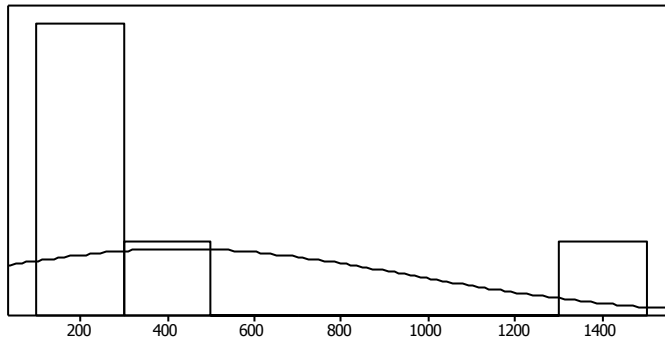
Test for Normality - Skin Removed (All Specimens)



t-test OK

Anderson-Darling Normality Test	
A-Squared	0.38
P-Value	0.279
Mean	184.67
StDev	90.64
Variance	8216.27
Skewness	0.981408
Kurtosis	0.287090
N	6
Minimum	104.00
1st Quartile	106.25
Median	167.50
3rd Quartile	253.00
Maximum	337.00
95% Confidence Interval for Mean	
	89.54 279.79
95% Confidence Interval for Median	
	105.07 297.00
95% Confidence Interval for StDev	
	56.58 222.31

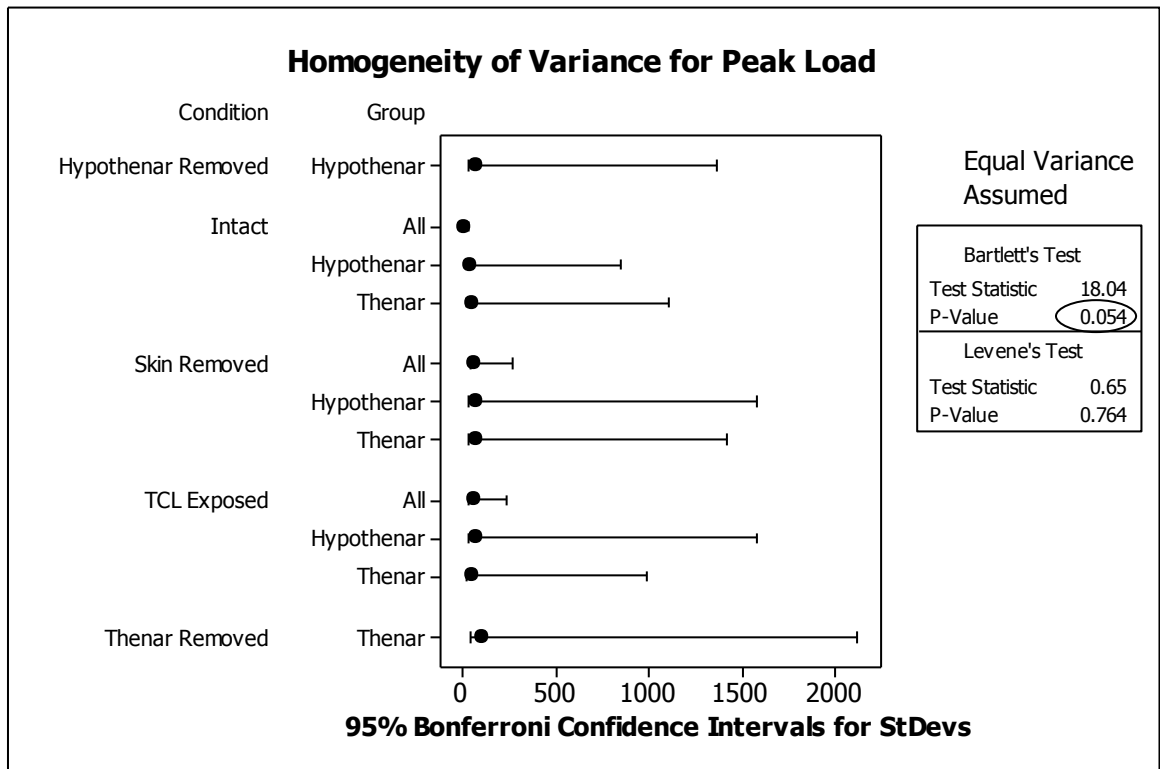
test for Normality - TCL Exposed (All Specimens)



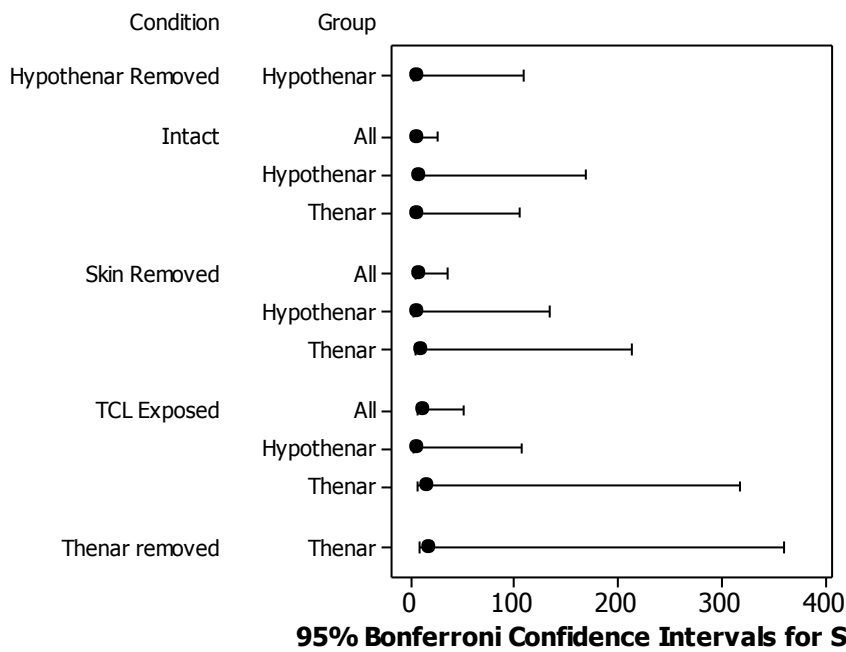
t-test NOT OK

Anderson-Darling Normality Test	
A-Squared	1.02
P-Value <	0.005
Mean	430.83
StDev	525.89
Variance	276563.77
Skewness	2.27211
Kurtosis	5.28183
N	6
Minimum	130.00
1st Quartile	139.75
Median	220.50
3rd Quartile	660.25
Maximum	1486.00
95% Confidence Interval for Mean	
	-121.06 982.72
95% Confidence Interval for Median	
	134.64 1092.79
95% Confidence Interval for StDev	
	328.27 1289.81

Appendix E Homogeneity of Variance graphs



Homogeneity of Variance for Stiffness

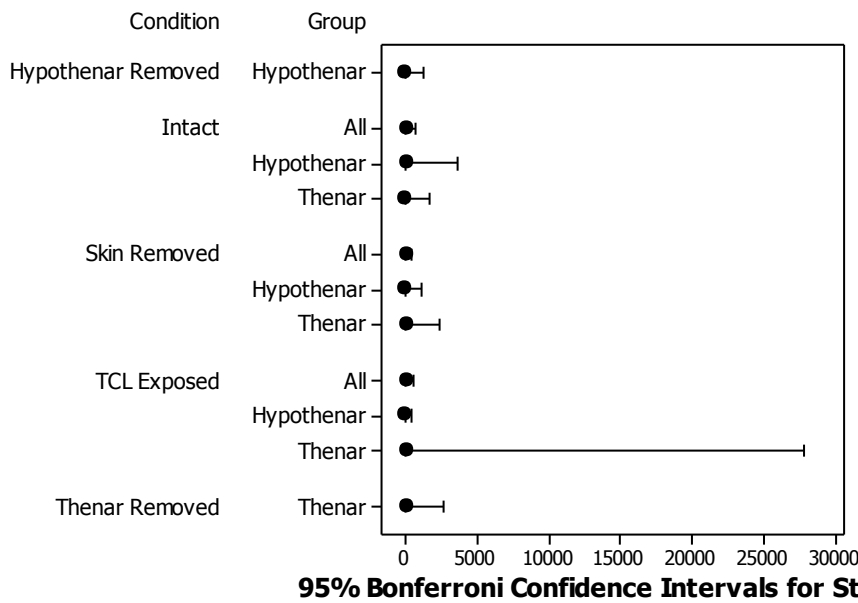


Equal Variance Assumed

Bartlett's Test	
Test Statistic	8.12
P-Value	0.617
Levene's Test	
Test Statistic	0.55
P-Value	0.844

95% Bonferroni Confidence Intervals for StDevs

Homogeneity of Variance for Relaxation Time

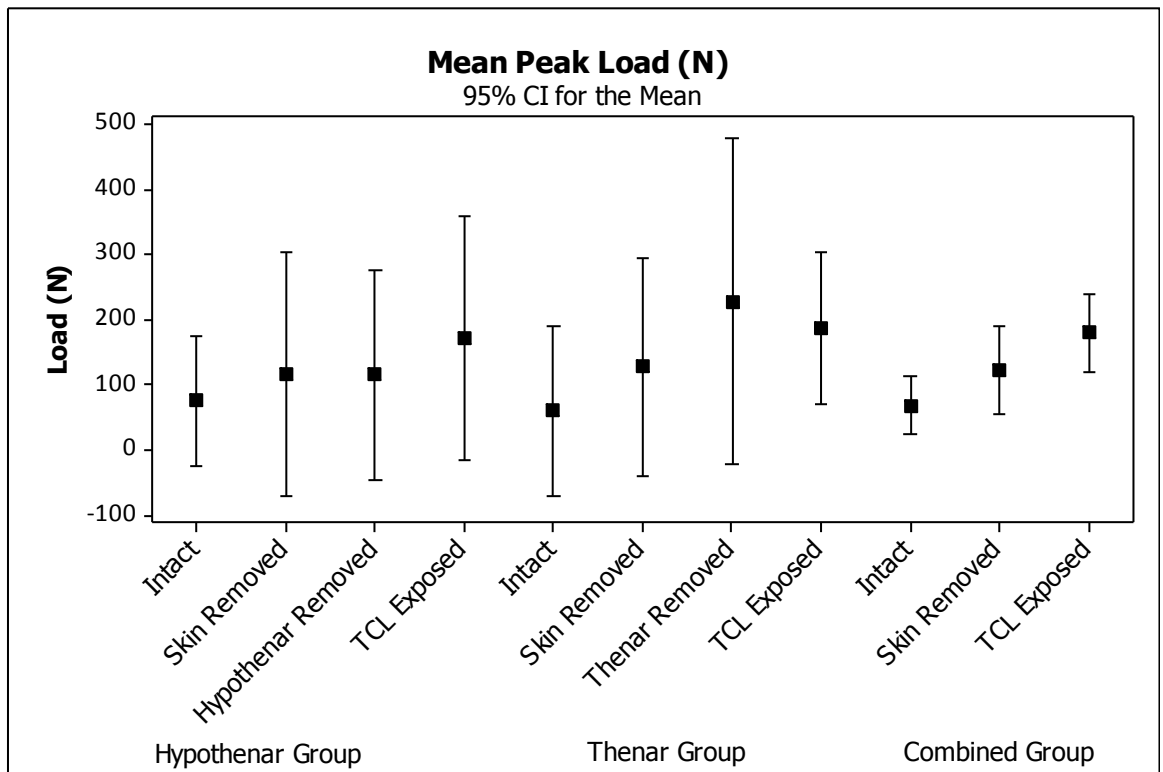


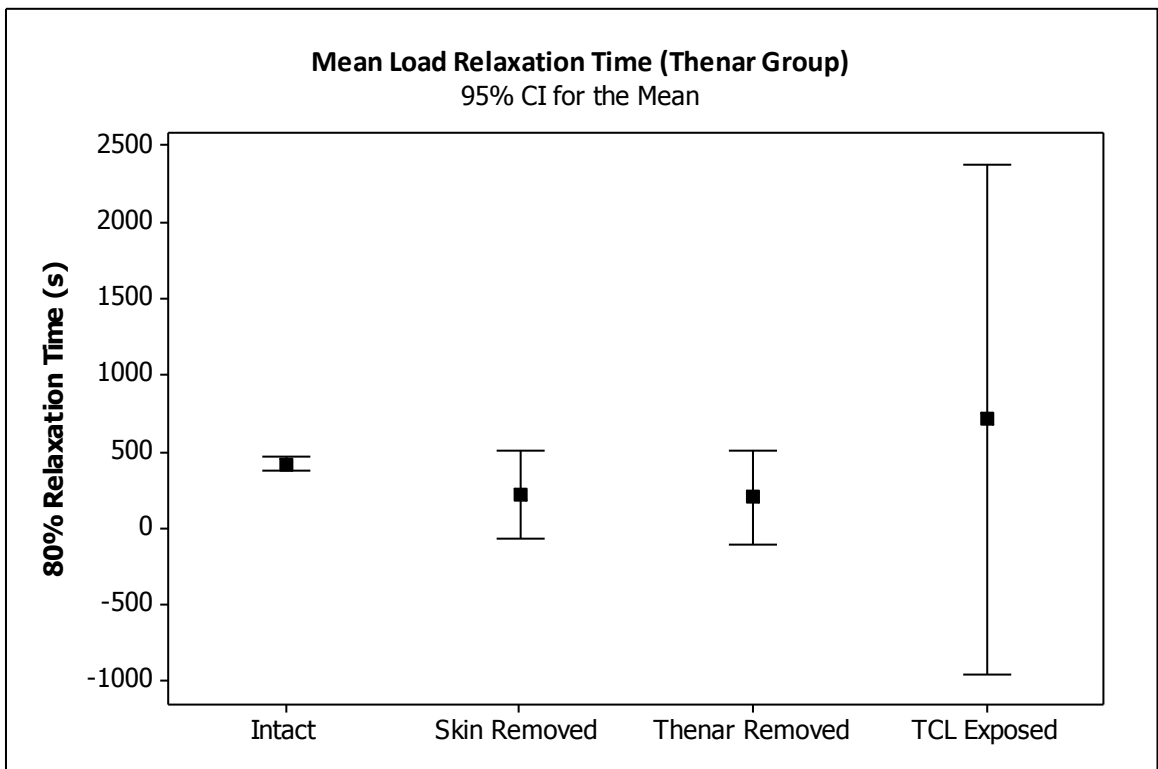
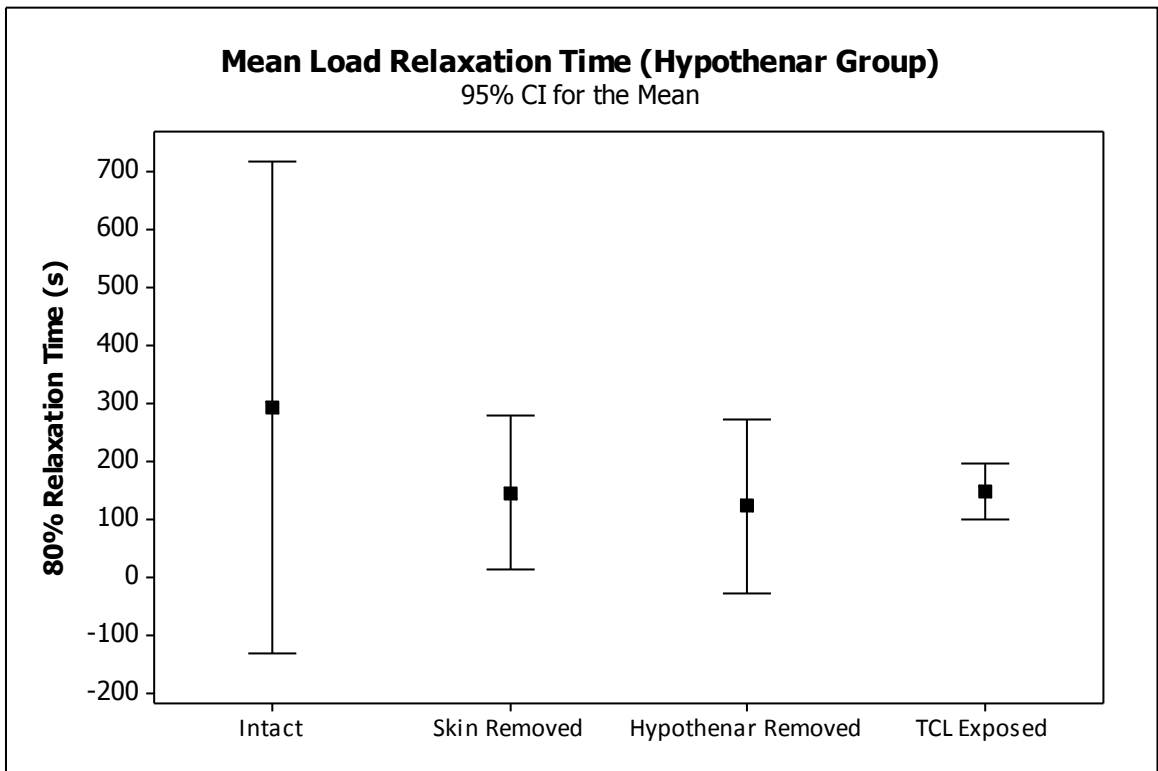
Equal Variance Assumed

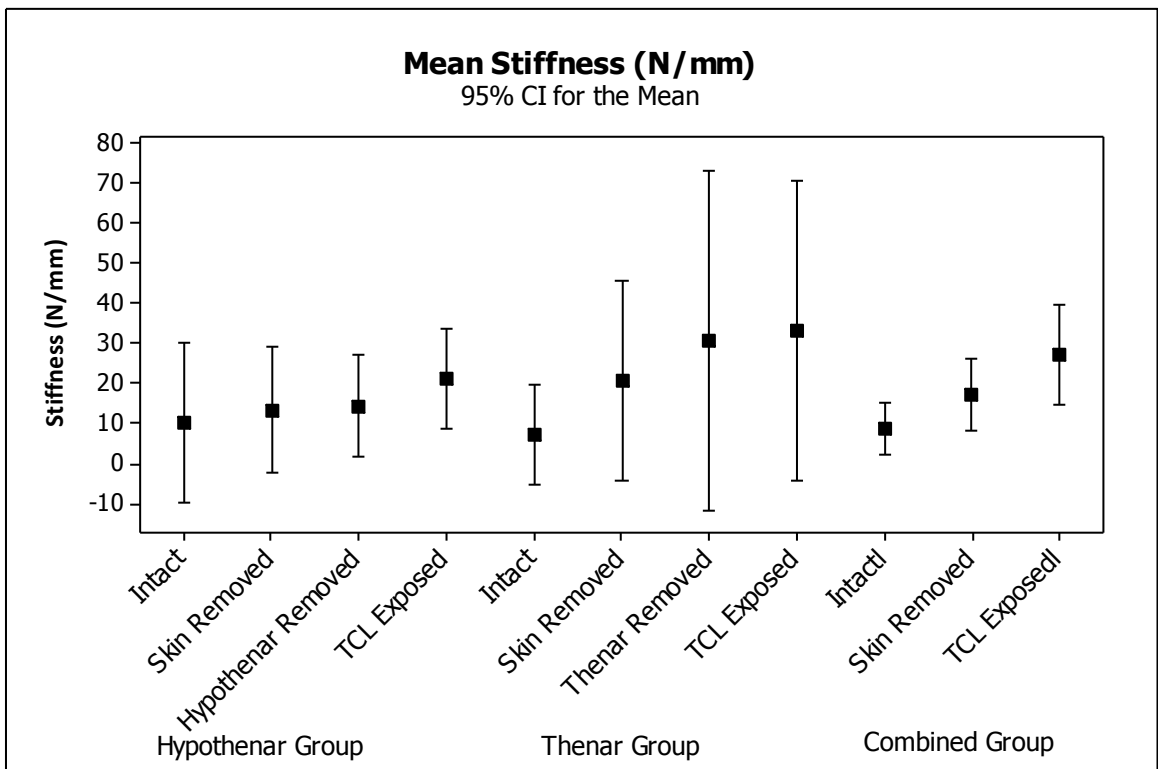
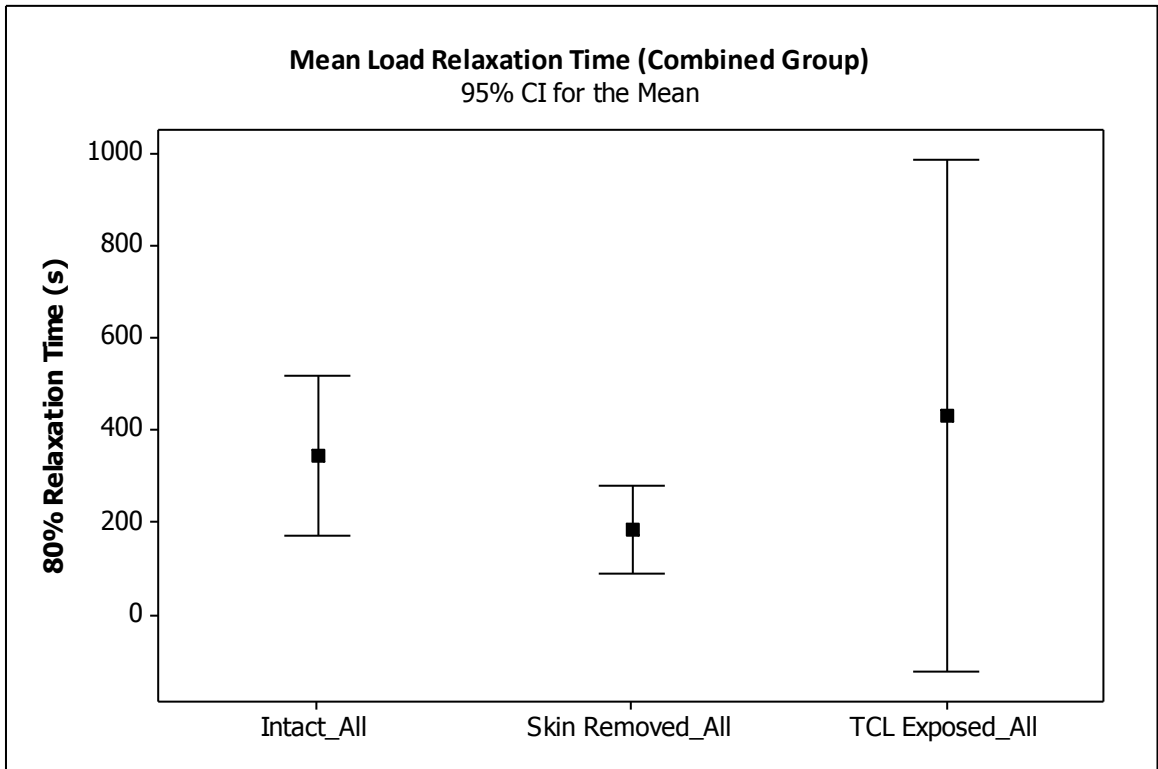
Bartlett's Test	
Test Statistic	12.35
P-Value	0.262
Levene's Test	
Test Statistic	0.49
P-Value	0.883

95% Bonferroni Confidence Intervals for StDevs

Appendix F: 95% Confidence Interval Graphs







Appendix G: Raw Anthropometric Measurements

Table 7: Individual specimen anthropometric measurements for the hand and wrist.

Specimen No.	Thenar or Hypo-thenar Group	Wrist Width	Wrist Thickness	Palm Width with Thumb	Palm Width	Palm Thickness	Palm Depth TCL Exposed	Tissue Layer Thickness
1	H	63.67	42.99	102.18	83.16	51.12	41.42	9.70
2	T	65.57	44.20	96.16	80.50	48.72	38.7	10.02
3	T	65.11	43.01	97.05	86.35	46.96	38.31	8.65
4	H	62.45	41.00	84.95	77.72	40.07	35.32	4.75
5	T	60.54	36.99	75.67	76.76	37.35	31.09	6.26
6	H	60.47	47.40	96.36	82.15	47.32	33.92	13.40
Mean		62.97	42.60	92.06	81.11	45.26	36.46	8.80
SD		2.20	3.46	9.82	3.57	5.35	3.73	3.04

Table 8: Individual specimen antropometric measurements; TCL dimensions

Specimen No.	Thenar or Hypo-thenar Group	Distal Thickness	Proximal Thickness	Distal Width	Proximal Width	Mid Width	Ulnar Length	Radial Length	Mid Length
1	H	1.82	1.17	23.72	28.95	22.99	22.39	22.59	20.46
2	T	1.55	1.59	25.21	29.42	29.27	20.88	19.68	16.83
3	T	1.51	1.56	18.67	23.75	23.68	20.06	18.94	17.45
4	H	1.58	1.06	22.7	24.43	21.67	25.74	22.02	20.34
5	T	1.54	1.1	27.23	26.29	25.11	22.97	19	16.38
6	H	2.15	1.72	25.44	28.32	27.84	22.4	20.45	16.03
Mean		1.69	1.37	23.83	26.86	25.09	22.41	20.45	17.92
SD		0.25	0.29	2.97	2.41	2.94	1.96	1.55	1.98